European Journal of Pharmaceutical Sciences 185 (2023) 106442

Contents lists available at ScienceDirect

European Journal of Pharmaceutical Sciences

journal homepage: www.elsevier.com/locate/ejps

A ready-to-use dry powder formulation based on protamine nanocarriers for pulmonary drug delivery

Sandra Robla [a], Rubén Varela Calviño [b], Rita Ambrus [c], Noemi Csaba [a,*]

[a] Center for Research in Molecular Medicine and Chronic Diseases (CiMUS) and Department of Pharmacology, Pharmacy and Pharmaceutical Technology, University of Santiago de Compostela, A Coruña, Spain
[b] Department of Biochemistry and Molecular Biology, University of Santiago de Compostela, A Coruña, Spain
[c] Faculty of Pharmacy, Institute of Pharmaceutical Technology and Regulatory Affairs, University of Szeged, Szeged, Hungary

ARTICLE INFO

Keywords:
Protamine nanocapsules
Rifabutin
Mannitol
Pulmonary drug delivery
Anti-tuberculotic treatment

ABSTRACT

The use of oral antibiotic therapy for the treatment of respiratory diseases as tuberculosis has promoted the appearance of side effects as well as resistance to these treatments. The low solubility, high metabolism, and degradation of drugs as rifabutin, have led to the use of combined and prolonged therapies, which difficult patient compliance. In this work, we develop inhalable formulations from biomaterials such as protamine to improve the therapeutic effect. Rifabutin-loaded protamine nanocapsules (NCs) were prepared by solvent displacement method and were physico-chemically characterized and evaluated for their dissolution, permeability, stability, cytotoxicity, hemocompatibility, internalization, and aerodynamic characteristics after a spray-drying procedure. Protamine NCs presented a size of around 200 nm, positive surface charge, and drug association up to 54%. They were stable as suspension under storage, as well as in biological media and as a dry powder after lyophilization in the presence of mannitol. Nanocapsules showed a good safety profile and cellular uptake with no tolerogenic effect on macrophages and showed good compatibility with red blood cells. Moreover, the aerodynamic evaluation showed a fine particle fraction deposition up to 30% and a mass median aerodynamic diameter of about 5 μm, suitable for the pulmonary delivery of therapeutics.

1. Introduction

Tuberculosis (TB) is an infectious disease caused by the Gram+ bacteria *Mycobacterium tuberculosis* (Mtb). TB's global mortality of 1.4 million people (WHO, 2019) constitutes a significant public health challenge (Chae et al., 2021). Pulmonary TB is the most characteristic form of disease, where Mtb, once inhaled, is phagocytosed by alveolar macrophages, multiplying and giving rise to an inflammatory reaction and characteristic tissue damage in the upper lobes of the lungs (Lado, 2002). TB treatment consists of 6 months of oral administration of the first-line drugs isoniazid, rifampicin, ethambutol, and pyrazinamide. A second-line TB treatment extends up to 9 or 20 months in case of isoniazid or rifampicin resistance, respectively, and includes the use of oral or parenteral drugs such as kanamycin, moxifloxacin or levofloxacin (Suárez et al., 2019). The oral route is the most suitable and least expensive for TB treatment, however, extended administration of high doses is required, and only sub-therapeutic levels of anti-TB drugs reach the site of action due to elevated first-pass metabolism and degradation (Sosnik et al., 2010). Compared to the oral route, the pulmonary route allows rapid action and higher bioavailability due to the large surface area and high vascularization of alveoli (70–140 m^2) for the achievement of high concentrations at the site of Mtb action, the alveolar macrophages (Chae et al., 2021), thereby reducing unwanted systemic effects. However, this route is constituted by a set of physical and biological barriers with complex geometry and high humidity, mucociliary clearance, or the presence of macrophages and alveolar enzymes which pose a great challenge for the administration of drugs (El-Sherbiny et al., 2015). Although studies of inhalation therapy for TB began in the late 1940s, after oral treatment began to show resistance (Traini and Young, 2017), they are still in preclinical development with no anti-tubercular inhalable formulation available in the market (Braunstein et al., 2019).

Rifabutin is a derivative of rifamycin, which has shown tolerability and safety in the treatment of disseminated intracellular infection by *Mycobacterium avium*, with significant advantages over rifampicin in the treatment of *M. tuberculosis* (Aristoff et al., 2010). It has shown a

* Corresponding author.
E-mail address: noemi.csaba@usc.es (N. Csaba).

https://doi.org/10.1016/j.ejps.2023.106442
Received 23 January 2023; Received in revised form 9 March 2023; Accepted 31 March 2023
Available online 3 April 2023

minimum inhibitory concentration *in vitro* and lower protein binding than rifampicin, with greater accumulation in cells and lipid solubility, which provides a larger volume of distribution (Davies et al., 2007). Therapeutic strategies based on nanotechnology offer the possibility of overcoming biological barriers and protecting biomacromolecules against degradation. The few reports available on rifabutin-based nanotechnology-based drug delivery systems comprised liposomes and solid lipid nanoformulations for intravenous, oral or pulmonary (Gaspar et al., 2016, 2008; Nimje et al., 2009; Nirbhavane et al., 2017) TB treatment, as well as Chron's disease (Rouco et al., 2020) or *M. avium* infection (Gaspar et al., 2000). However, upon pulmonary administration their nanometric size results on low inertia, which carries the risk of exhalation (up to 80%) without being deposited in the airways (Yang et al., 2008). Recent advances in particle engineering and materials science have opened a door for improving the efficacy of inhalation by the production of porous microparticulate powders with the optimal size for drug deposition at the targeted site (El-Sherbiny et al., 2015). Microparticle administration in the form of dry powder inhalers (DPIs) constitutes a promising strategy, with highly effective drug lung deposition and patient adherence (Nainwal et al., 2022). The controlled agglomeration of nanoparticles into micron-sized particles has been used as an effective delivery method using DPIs. These platforms act as an intermediate delivery system until reaching the alveoli, where the redispersion of the agglomerates of nanoparticles occurs, causing their release (Malamatari et al., 2020). The present study aimed to design and develop a drug delivery system to overcome the limitations related to anti-tuberculosis therapy. Rifabutin was encapsulated into protamine nanocapsules, and formulations were characterized and spray-dried with mannitol for the obtention of a DPI. The present work demonstrates the potential of the developed nanocarriers evaluating their distribution in the lung and showing their suitability for pulmonary administration.

2. Experimental section

2.1. Materials

Rifabutin was acquired from Chemos GmbH (Germany). Low molecular weight protamine sulfate (5 kDa) was purchased from Yuki Gosei Kogyo, Ltd (Japan). Polyethylene glycol stearate 40 (PEGst 40) was provided by Croda Chemicals Europe Ltd. (United Kingdom) and sodium glycocholate (SGC) was purchased from Dextra laboratories Ltd. (United Kingdom). Caprylic/capric/succinic triglyceride (Miglyol® 812) was obtained from IOI Oleo GmbH (Germany). D-Mannitol was obtained from Molar Chemical KFT (Hungary). 3-(4,5-dimethyl-2-thiazolyl)-2,5-diphenyl-2H-tetrazolium bromide (MTT) and 4,6-diamidino-2-phenylindole (DAPI) dye were purchased from Sigma-Aldrich (St. Louis, MO, USA). 1,1′-Dioctadecyl-3,3,3′,3′-tetramethylindodicarbocyanine, 4-chlorobenzenesulfonate salt (DiD) was provided by Thermo Fisher Scientific (USA). Ficoll-Paque™ PLUS was obtained from GE Healthcare Bio-Science AB, (Sweden), Medium Roswell Park Memorial Institute (RPMI-1640), and Dulbecco's Modified Eagle's Medium (DMEM) were obtained from GIBCO® (Thermo Fisher Scientific, Spain). Granulocyte-macrophage colony-stimulating factor (GM-CSF) was obtained from Tonbo Biosciences (San Diego, CA, USA). Fetal Bovine Serum (FBS), and PSG (Penicillin-Streptomycin-Glutamine) were provided by Sigma Aldrich. A549 human alveolar lung carcinoma cell line and Raw 264.7 cell line were obtained from ATCC (Manassas, VA, USA). Sodium chloride (NaCl), sodium hydrogen carbonate ($NaHCO_3$), glycine ($C_2H_5NO_2$), calcium chloride dihydrate ($CaCl_2$), sulfuric acid (H_2SO_4) and sodium phosphate hydrated (NaH_2PO_4 H_2O) were purchased from Sigma Aldrich (St. Louis, MO, USA), Trifluoroacetic acid was obtained from Merck Schuchardt OHG (Germany). All other reagents were of analytical grade and were used without further purification.

2.2. Preparation and characterization of protamine nanocapsules

Protamine nanocapsules were prepared by solvent displacement technique following the procedure described by our group, with modifications (Thwala et al., 2016). An oily core of 29.5 mg of Miglyol®812, 2.5 mg of SGC, 8 mg of PEGst-40 an acetone up to a final volume of 2.5 mL was poured over 5 mL of an aqueous phase of 0.15% protamine, and the formulation was left under magnetic stirring at 1000 rpm for 10 min. The organic solvents were evaporated under vacuum in a Rotary Evaporator (Rotavapor R-215, Büchi, Switzerland) and finally, nanocapsules were isolated by centrifugation (Hermle Labnet universal centrifuge Z323K, Labnet international) at 15,000 g at 15 °C for 1 h. The isolated formulation was resuspended in ultrapure water. For the preparation of rifabutin-loaded protamine nanocapsules, rifabutin was dissolved in acetone (1, 2.5, and 5% of theoretical drug over total nanocapsules weight) and incorporated into the liquid lipid phase prior to nanocapsule formation.

Blank and rifabutin-loaded protamine nanocapsules were optionally freeze-dried for 48 h using Scanvac, Coolsafe 100–9 apparatus (LaboGeneApS, Lynge, Denmark) including mannitol in a ratio of 80/20 (w/w) as a cryoprotectant. Subsequently the nanoparticles process yield was calculated by gravimetry:

$$\text{Process yield (Y\%)} = \frac{\text{Weight of nanocapsules}}{\text{Theoretical weight of nanocapsules}} \text{x } 100$$

Nanocapsules were characterized in terms of mean particle size (nm), polydispersity index (PDI), and Z potential (mV) using photon correlation spectroscopy (Zetasizer Nano-ZSTM, Malvern Panalytical), after dilution in ultrapure water (dilution 1:250 at 25 °C and with a detection angle of 173°) and Nanoparticle Tracking Analysis (NTA, NanoSight 142 NS3000, Malvern analytical Ltd., Malvern, UK). For NTA analysis, NCs were diluted 1:1000 in order to keep the concentration within the instrument measuring range.

The morphology of the nanocapsules (dilution 1:1000) was analyzed by field emission scanning electron microscopy (FESEM; Gemini-SEM, Zeiss, Germany) after coating the samples with iridium in an argon atmosphere.

Lyophilized protamine NCs were characterized by Fourier Transform infrared spectroscope (FTIR) (Thermo Nicolet AVATAR 330, Waltham, MA, USA) at 4 cm^{-1} resolution at the wavenumber range of 400–4000 cm^{-1}. The crystallinity of the NCs was evaluated by X-Ray Powder Diffraction (XRPD) using a Bruker D8 Advance X-ray diffractometer (Bruker AXS GmbH, Karlsruhe, Germany). The XRPD and FTIR spectra were analyzed using OriginPro 2017 (OriginLab Corporation, USA) and Spectragryph v1.2.16.1 software, respectively.

2.3. Encapsulation efficiency and drug loading

Associated rifabutin was quantified using an Acquity UPLC H-Class Plus system equipped with a C_{18} column (Waters® symmetry 1.7 μm, 2.1 × 50 mm) adapting a protocol developed by Rouco et al. (2020). Briefly, 10 μL of each sample were injected and eluted with a mobile phase composed of (A) a mixture of sodium acetate 0.05 M/potassium dihydrogen phosphate 0.05 M (pH adjusted to 4.0 with acetic acid) and (B) acetonitrile in a ratio A:B 53:47 (v/v). Drug quantification was performed at a wavelength of 278 nm, with a 0.2 mL/min flow rate. The Limit of Detection (LOD) was 0.016 ng/mL and the Limit of Quantification (LOQ) was 0.048 ng/mL, with a retention time of 1.7 min. Rifabutin was analyzed in the range of 5–35 μg/mL, showing a correlation coefficient of R= 0.9997. NCs were dissolved with a mixture of acetonitrile/sodium acetate/potassium dihydrogen in the same ratio as the mobile phase and centrifuged (Eppendorf 5430R®) at 12,000 g and 4 °C for 30 min for drug isolation. This procedure was repeated, and samples were filtered before UPLC measurement by 0.22-micron syringe filters. The rifabutin encapsulation efficiency (EE%) and drug loading (DL%) in protamine nanocapsules were calculated according to the following equations:

$$\text{Encapsulation efficiency (EE\%)} = \frac{\text{Weight of initial drug} - \text{Weight of free drug}}{\text{Weight initial drug}} \text{x } 100$$

$$\text{Drug loading (DL\%)} = \frac{\text{Weight of loaded drug}}{\text{Weight lipid core}} \text{x } 100$$

2.4. Colloidal stability of the nanocapsules

The colloidal stability of rifabutin-loaded protamine NCs were evaluated in aqueous suspension under storage at 4 °C and in freeze-dried form at room temperature (RT) for 30 days. Stability was also evaluated in cell culture media and simulated lung media (SLM, pH 7.4) composed of 116 mM NaCl, 27 mM $NaHCO_3$, 5 mM $C_2H_5NO_2$, 1.1 mM NaH_2PO_4 (H_2O), 0.18 mM $CaCl_2$ and 0.5 mM 0.1 M H_2SO_4 in distilled water at pH 7.4 (Parlati, 2008). The mean particle diameter (nm), PDI, derived count rate (kcps) and zeta potential (mV) were analyzed using Zetasizer Nano-ZS™ as described in Section 2.2.

2.5. In vitro dissolution studies

In vitro dissolution studies were performed in simulated lung medium (SLM) to evaluate the release kinetics of rifabutin from the nanocapsules. The nanopowder quantity equivalent to 0.75 mg of rifabutin was dispersed in 10 mL of SLM. The stirring was adjusted at 200 rpm and the sampling was performed up to 1 h at 37 °C. 1 mL of the dissolution medium was collected into microcentrifuge tubes (Eppendorf) at time intervals of 5, 10, 15, 20, 30, 40, 50, and 60 min and replaced every time with fresh medium upon sample withdrawal. Release samples were centrifuged at 7,500 *g* and the collected supernatant was analyzed spectroscopically by using a UV–visible spectrophotometer (V-730 UV-visible Spectrophotometer, Jasco Deutschland) at a wavelength of 237 nm. All experiments were conducted in triplicate. The kinetics of the *in vitro* drug release were evaluated to Zero Order, First Order, Higuchi, and Korsmeyer–Peppas to understand the drug release mechanism.

2.6. In vitro permeability studies

The permeability study of rifabutin was performed on a modified horizontal diffusion side-by-side cell-type apparatus (Grown Glass, New York) (Gieszinger et al., 2021). Briefly, 9 mL of phosphate buffer (pH 7.4) was used in the acceptor chamber while the same volume of simulated lung media was used as donor media. Subsequently, 0.75 mg of raw rifabutin and rifabutin-loaded nanocapsules equivalent to 0.75 mg of rifabutin were dispersed into the donor chamber. Chambers were separated by an artificial membrane (Isopore™ membrane filter, 0.45 μm) impregnated in isopropyl myristate, with a diffusion area of 0.69 cm^2. The temperature was kept at 37 °C and stirred at 100 rpm. The amount of rifabutin diffused from protamine nanocapsules in the acceptor phase was measured for 1 h spectrophotometrically at 238 nm using a FDP-7UV200 probe and a Avaspec-ULS2048-USB2 spectrophotometer (Avantes, Apeldoorn, The Netherlands). The flux (J) (μg/cm^2/h) of rifabutin was calculated from the amount of drug (μg) permeated through the side-by-side membrane (m), divided by the surface of the membrane (A) and the time (t) following the equation:

$$J = \frac{m}{A * t}$$

The permeability coefficient (Kp) (cm/h) was determined from the flux and the initial rifabutin concentration in the donor phase (Cd) (g/cm^3), according to the equation:

$$Kp = \frac{J}{Cd}$$

2.7. In vitro toxicity studies

The cytotoxicity of rifabutin-loaded protamine nanocapsules was evaluated using MTT reduction, a water-soluble tetrazolium dye that is converted by viable cells to a water-insoluble and purple compound, formazan. Cell viability was assessed in A549 and Raw 264.7 cells after 24 h of incubation of different concentrations of nanocapsules. The day before the experiment, cells were seeded in a 96-well plate in DMEM culture medium supplemented with 10% FBS, and 1% Penicillin/Streptomycin at a cell density of 1×10^4 cells/well at 37 °C and 5% CO_2. On the next day, the medium was replaced by medium containing the formulations, and cells were incubated for 24 h. Fresh medium was used as the negative control and Triton x100 (1% v/v) was used as the positive control. After 24 h, the medium was replaced by 0.5 mg/mL of MTT dissolved in PBS, and cells were incubated for 4 h at 37 °C and darkness. MTT solution was discarded, and the formazan crystals were dissolved by the addition of 0.04 N HCl in isopropanol. Absorbance was measured at 570 nm using a microplate reader (Synergy H1 Hybrid Multi-Mode, BioTek, Winooski, VT, USA). Cells treated with equivalent rifabutin concentrations were used as control. The cell viability (%) compared to control cells was calculated following the equation:

$$\text{Cell toxicity (\%)} = \frac{\text{Absorbance sample} - \text{Absorbance positive control}}{\text{Absorbance negative control} - \text{Absorbance positive control}} \text{x } 100$$

2.8. Quantitative nanocapsules uptake

Rifabutin-loaded protamine nanocarriers were labeled by incorporating 20 μL DiD (2.5 mg/mL) in ethanol into the organic phase prior to nanocapsule formation. Physicochemical characterization and drug loading were evaluated to confirm that the dye did not interfere with the physico-chemical properties of the formulation before *in vitro* assays.

A549 and Raw 264.7 cells were grown in 8-μwell slides ibidiTreat (Ibidi GmbG, Gräfelfing, Germany) (0.8 cm^2/well) at 2.5×10^4 cells/well and DiD-labeled rifabutin-loaded protamine NCs were added and incubated for 24 h. Then, formulations were removed with PBS pH 7.4 (x3) and cells were fixed with 4% paraformaldehyde (PFA) for 15 min at RT and 150 rpm. Then, PFA was removed with PBS (x3) and the nucleus was stained with DAPI for 5 min. Finally, cells were washed with PBS (x3) and mounted in glycerol. Nanocapsules internalization was studied by Confocal Laser Scanning Microscopy (CLSM, SP5 Leica AOBS-SP5, Leica Biosystems Nussloch GmbH). Fluorescence measurements were performed at DAPI-dye excitation λ_{max}= 359 nm and emission λ_{max}= 457 nm

and DiD-dye excitation λ_{max}=640 nm and emission λ_{max}= 675 nm.

To quantify the A549 cells and Raw 364.7 internalized with rifabutin-loaded protamine NCs, a study based on flow cytometry was carried out. 6×10^4 cells were seeded in a 24-well plate at 37 °C for 24 h and 5% CO_2. The medium was replaced with formulations and cells were incubated for 24 h, washed with PBS and detached with trypsin (5 min, 37 °C). Cells were centrifuged at 1,000 g (Eppendorf 5430R®) for 10 min, and the pellet was resuspended in 500 μL PBS. Non-treated cells were used as negative control. Events were counted employing a cytometer (BD FACSCalibur™, Becton Dickinson) and were analyzed by flowing software 2.5.1 (Cell Imaging Core, Turku centre for Biotechnology). The study was carried out in triplicate.

2.9. IDO assay

Tolerogenic phenotype of the developed rifabutin-loaded protamine NCs was evaluated on human-derived macrophages in terms of T cell suppression and tolerance promotion by quantification of 2,3-Indoleamine dioxygenase (IDO) expression. Buffy coats were donated by the Organ and Blood Donation Agency (ADOS; Santiago de Compostela, Spain) after informed consent. Briefly, the blood was diluted with PBS (1:1) and peripheral blood mononuclear cells (PBMCs) were isolated using the Ficoll density gradient separation method (blood/Ficoll ratio of 2:1) by centrifugation (Allegra X-12R, Beckman Coulter) at 400 g for 30 min at RT on deceleration mode. Red Blood Cells (RBCs) were kept for blood compatibility assays (Section 2.10.) and the PBMC layer was washed with PBS by centrifugation at 300 g for 10 min. 10 mL of the obtained cells (1.2×10^6 cells/mL) were then resuspended in a R_2 media (RPMI-1640 supplemented with 2% FBS and 1% of Penicillin-Streptomycin-Glutamine, PSG) for 2 h (37 °C, 5% CO_2). After this time, the non-adherent cells, peripheral blood lymphocytes, were washed with PBS. The attached monocytes were cultured for 6 days in R_{10} media (RPMI-1640 supplemented with 10% FBS and 1% of PSG), replacing the media on the third day and adding 0.1 μg GM-CSF for the differentiation of monocytes to macrophages.

Macrophages were seeded onto a 48-well plate, followed by their incubation with different formulations in a final volume of 0.5 mL and by adding 1.25 μL of L-tryptophan (100 μM) 4 h before the end of the culture period. After 24 h, cells were centrifuged (1,000 g, 5 min at RT) and supernatants were mixed with 30% trifluoroacetic acid (2:1 v/v). Cells were centrifuged again and Ehrlich Reagent (1:1 v/v) was added to the supernatant. Absorbance was read using a microplate reader (Synergy H1 Hybrid Multi-Mode, BioTek, Winooski, VT, USA) at 490 nm. A total of 3 different donors were used and were plotted along with the standard error.

2.10. Blood compatibility test

As described in Section 2.9., after the Ficoll density gradient separation method, freshly collected RBCs were collected, washed with PBS (x3, pH 7.4), and centrifuged at 1,000 g for 5 min at RT. The RBC pellet was resuspended in PBS and placed in a 96-well plate and was treated with rifabutin-loaded protamine NCs (0.1 mg/mL) at 37 °C for 4 h and 24 h. Triton x100 (1% v/v) was used as the positive control while PBS was used as the negative control. A total of 3 different donors were used and results were plotted along with the standard error. At signaled time points the absorbance of released hemoglobin was measured at 570 nm (Synergy H1 Hybrid Multi-Mode, BioTek, Winooski, VT, USA), and percentage hemolysis was calculated using the following equation:

$$\%\ \text{Haemolysis} = \frac{\text{Absorbance sample} - \text{Absorbance negative control}}{\text{Absorbance positive control} - \text{Absorbance negative control}} \text{x } 100$$

2.11. Thermal analysis

The influence of temperature on the physicochemical properties of rifabutin-loaded protamine NCs was evaluated by DLS. Samples (dilution 1:250) were placed in a quartz cell and particle size, PDI, and count rate measurement was performed by heating the sample from 25 °C up to 90 °C at a heating rate of 1 °C/min. Measurements were performed in triplicate.

2.12. Preparation of dry powders containing rifabutin protamine nanocapsules

Mannitol was used as an excipient for dry powder preparation and samples were spray-dried using the Nano Spray Dryer B-90 HP Nano SD (Büchi Labortechnik AG, Falwil, Switzerland) with an inlet air temperature of 100 °C, an outlet T^a of 31 °C a pump flow rate of 20%, and aspirator capacity of 100%. Protamine nanocapsules were suspended in an aqueous solution of mannitol to achieve a theoretical mannitol/nanocapsules ratio of 80/20 (w/w) (Grenha et al., 2007) and a final solid content of 1.25% (w/v), as it is expected to lead to the production of microparticles with adequate morphologic and aerodynamic characteristics for pulmonary administration. The spray-dried powders were stored in a desiccator at RT until use. Samples were analyzed by Differential Scanning Calorimetry (DSC) was performed using a Mettler-Toledo 821e DSC (Mettler-Toledo GmbH, Gießen, Germany) at the temperature interval of 30 to 450 °C under constant purging of argon. DSC spectra were analyzed using the STARe thermal analysis program V9.1 (Mettler Inc., Schwerzenbach, Switzerland). The crystallinity was also evaluated by XRPD using a Bruker D8 Advance X-ray diffractometer as described in Section 2.2. The spray-dried particles were dissolved in water to achieve in-water dispersed rifabutin-loaded protamine NCs and were subsequently evaluated by dynamic light scattering as previously described in Section 2.2. The morphology of the spray-dried nanocapsules was analyzed by scanning electron microscopy (SEM) (Hitachi S4700, Hitachi Scientific Ltd., Tokyo, Japan) after coating the samples with gold-palladium in an argon atmosphere.

2.13. In vitro aerodynamic evaluation

The *in vitro* distribution profile of the spray-dried protamine NCs was evaluated using the Andersen cascade impactor (ACI, Copley Scientific Ltd., Nottingham, UK). The used methodology respected the United States Pharmacopeia and Ph. Eur. 2.9.18 requirements. ACI separates particles according to their aerodynamic diameter by cut-offs of the stages from −1 to 6 (8.60, 6.50, 4.40, 3.20, 1.90, 1.20, 0.55, and 0.26 μm). A glass fiber filter (Pall corporation, Mexico, 1.0 μm pore size and aerosol retention of 99.98%) was placed right below stage six. Collection plates were coated with Span 80 + cyclohexane solution (1 + 99 w/w %) to prevent particle bounce. An amount of 8 mg of spray-dried protamine NCs was loaded into 4 hard gelatin capsules (transparent, size 3, Capsugel, Germany) and aerosolized using a DPI Breezhaler® single dose device (Novartis International AG, Basel, Switzerland). The content of the four capsules was discharged for each experiment, and the experiments were performed in triplicate. The flow rate was adjusted at 60 L/min using a DFM 2000 Flow Meter (Copley Scientific, Nottingham, UK), and the test duration time was adjusted at 4 s. The DPI device, the mouthpiece, the induction port, the eight stages of the impactor, and the end filter were weighed before and after the experiment, and parameters (MMAD, FPD, ED, and FPF) were quantified by gravimetry. The *in vitro*

aerodynamic properties were evaluated with Inhalytix™ (Copley Scientific LTD., Nottingham, United Kingdom) data analysis software.

Mass median aerodynamic diameter (MMAD) was determined by plotting the cumulative percentage of mass for each stage on a probability scale *versus* the aerodynamic diameter of the stage on a logarithmic scale. The fine particle dose (FPD) corresponded to the mass of particles with a size <5 μm, fine particle fraction (FPF) was established as the percentage of particles <5 μm, while emitted dose (ED) was the percentage of particles leaving the device and reaching the impactor. Time-of-flight (TOF) particle size analyzer Aerosizer® (TSI Instruments Ltd. UK) connected with Aero-Disperser® was also used to confirm the aerodynamic size distribution by timing the flight of the individual spray-dried nanocarriers. A small amount of powder (around 5 mg) was placed in the sample cup of the aerodisperser and measurements were performed using laser current 41 mA, a nozzle type 200 μm, a size range from 0.1 to 200 μm and a run length of 30 s.

2.14. Statistical analysis

The statistical significance of the difference between the means was determined by GraphPad Prism 8 and OriginPro 9.0. All data are shown as mean±SD or mean± SEM (IDO and hemolysis assay) and one-way and two-way analyses of variance (ANOVA) were performed to compare multiple independent groups. Differences were considered statistically significant at $P < 0.05$.

3. Results and discussion

3.1. Preparation and characterization of rifabutin protamine nanocapsules

In this work, we use protamine, a natural arginine-rich polypeptide with remarkable stability in simulated biological fluid, widely used in the design of polymeric nanocarriers for drug and vaccine delivery (Jakubiak et al., 2017). The attachment of protamine to the oily core was possible after the incorporation of an anionic surfactant, and the developed protamine nanocapsules were stabilized by incorporating PEG-stearate. The different rifabutin formulations were prepared at theoretical loadings of 1%, 2.5%, and 5% (w/w) (Supplementary Fig. 1). To evaluate the incorporation of rifabutin in the oily phase of the nanocapsules, nanoemulsions were first analyzed by DLS and UPLC (Supplementary Table 1), and then, protamine nanocapsules were prepared by solvent displacement technique. The mean hydrodynamic diameter of unloaded and rifabutin-loaded protamine nanocapsules is presented in Table 1 and was found to be around 200 nm for all formulations. No statistical differences were observed between loaded and unloaded nanocapsules, suggesting that rifabutin incorporation does not influence the particle diameter and surface charge, which was found to be positive (from +11 to +17 mV). It has been shown that a hydrodynamic diameter > 100 nm and a positive surface charge significantly improve the particle-macrophage interaction and internalization, since phagocytic activity depends on particle size and macrophages present sialic acid on their surface, which gives them a negative surface charge (Lee et al., 2015). In all cases, high rifabutin incorporations were obtained, as shown in Table 1. The satisfactory encapsulation as well as the high yields achieved (up to 90%) confirm the suitability of the developed nanocarriers for rifabutin incorporation.

Table 1
Physicochemical characterization, association efficiency (AE), and Drug Load (DL) of non-loaded and rifabutin-loaded (1, 2.5, and 5%) protamine nanocapsules (NCs). Particle hydrodynamic diameter and polydispersity index (PDI) were obtained by Dynamic Light Scattering. Data represents mean ± SD, N>3.

Formulation	Size (nm)	PDI	Charge (mV)	AE (%)	DL (%)	Yield (%)
Blank NCs	199 ± 17	<0.2	11 ± 10	–	–	91 ± 2
1% Rifabutin NCs	185 ± 13	<0.2	9 ± 10	54 ± 18	0.87	79 ± 19
2.5% Rifabutin NCs	199 ± 15	<0.2	9 ± 8	46 ± 6	1.88	91 ± 4
5% Rifabutin NCs	198 ± 19	<0.2	11 ± 10	42 ± 7	3.55	86 ± 3

Their structural characterization is represented in Fig. 1 after their lyophilization process in the presence of mannitol. As shown in the FTIR spectrum (Fig. 1A), the developed nanocapsules presented the typical signal of protamine sulfate at around 1100–1150 cm^{-1} attributed to arginine (that constitutes 67% of the total amino acid content of protamine) (Awotwe-Otoo et al., 2012), as well as D-Mannitol δ-phase bands at 931, 967, 1023, 1086 and 1193 cm^{-1} (Barreneche et al., 2013). Moreover, characteristic bands of glycocholate acid were observed at 1582 and 1394 cm^{-1} (COO- stretching), 1308 (C−H bending) and 1037 cm^{-1} (ammonium stretching vibration) (Benbow et al., 2021). C-H scissor and bending at the region between 1450 and 1292 cm^{-1}, can be attributed to PEG-stearate 40 (Khairuddin et al., 2016). XRPD diffractogram (Fig. 1B) of rifabutin showed a distinctive drug sharp peak, indicative of the crystalline nature of rifabutin, whereas it faded away in the diffractogram of rifabutin-loaded protamine NCs. This reduction in relative integrated intensity of peak, with no distinct peak of rifabutin, suggests that drug was entirely incorporated into the oily core of the nanocapsules. In addition, it is indicative of amorphous material, which had shown to increase solubility compared to crystalline material (Nighute and Bhise, 2009).

A uniform shape, smooth surface and spherical morphology were observed by FESEM microscopy (Fig. 2 without aggregation of the nanocapsules. The NTA analysis further supported the above disclosed DLS and FESEM data and similar hydrodynamic particle sizes were reported (between 132 and 148 nm), slightly lower than those obtained by DLS measurement.

3.2. Stability studies

The size of the nanocarriers remained unchanged upon storage in suspension, and no signs of aggregation were observed for 30 days nor after the freeze-drying process. Mannitol was included as an inert carrier and stabilizer in the process, and it was completely dissolved after incubation of the lyophilized nanocapsules in an aqueous medium, inducing no significant changes in their physicochemical characteristics. The slight increase in zeta potential as compared with non-lyophilized nanocapsules, indicative of the stability of the colloidal system, was also reported previously for chitosan nanoparticles recovery from mannitol dry powders (Grenha et al., 2005) (Table 2).

SLM was prepared based on a modification of Gamble's original solution (Parlati, 2008) and was suitable for flow through dynamic systems. Following a protocol developed by Kanapilly et al., glycine was included to prevent clogging of filter pores in a dynamic flow system (Kastury et al., 2017). When incubated in SLM and cell culture media (Fig. 3), rifabutin-loaded protamine NCs exhibited satisfactory stability over time. In addition, the derived count rate (kilo counts per second, kcps) provided information about the concentration of nanoparticles remaining *in situ* in suspension after incubation and its degradation (Woods et al., 2020). Results showed no reduction in intact particle number following exposure to the cell culture media or SLM up to 24 h, strongly suggesting efficient physical and biological stabilization mechanisms of the developed formulations.

3.3. In vitro dissolution studies

To predict the *in vivo* efficacy of the formulations, an *in vitro* release of rifabutin from protamine NCs was performed in simulated lung media and results were analyzed using drug release kinetics models. *In vitro* rifabutin release from 1% loaded protamine NCs presented a drug

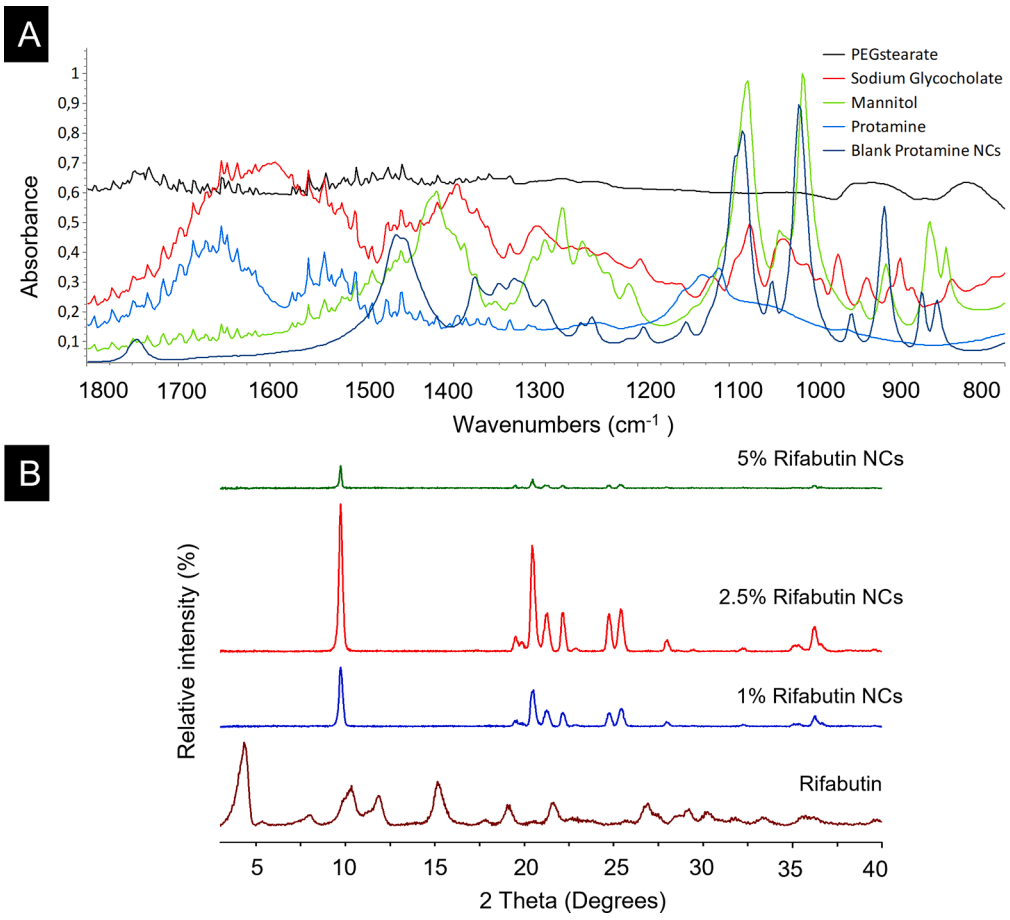

Fig. 1. (A) FTIR spectra of lyophilized protamine nanocapsules (NCs) and their components and (B) XRPD spectra of rifabutin and 1, 2.5, and 5% rifabutin-loaded protamine NCs.

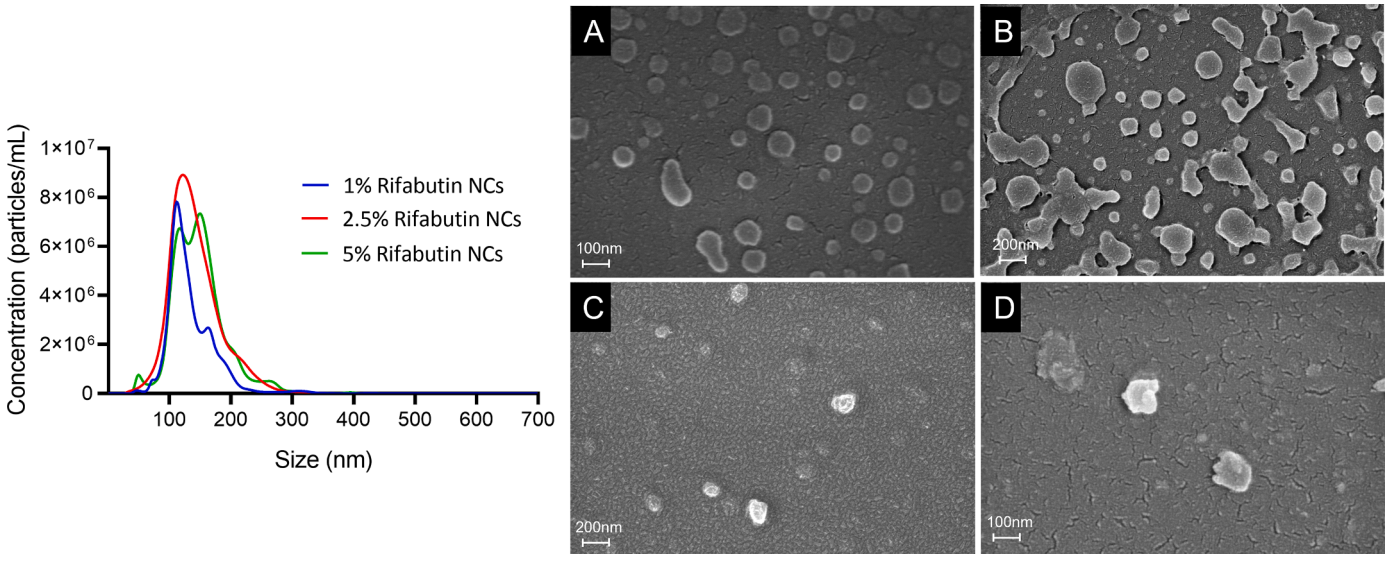

Fig. 2. (Left) Representative image of the particle size distribution by Nanoparticle Tracking Analysis of nanocapsules in solution and (Right) scanning electron microscopy images of blank (A) and rifabutin-loaded 1 (B), 2.5 (C) and 5% (D) protamine nanocapsules. Scale bars represent 100 nm.

release profile where all encapsulated rifabutin was released (96 ± 13%), while in the case of 2.5 and 5% rifabutin-loaded protamine NCs was of 71 ± 12 and 66 ± 27%, respectively, over 1 h (Fig. 4). Rifabutin dissolution was statistically significant (one way ANOVA $P < 0.05$) for 1% rifabutin protamine NCs when compared with raw drug dissolution. Formulations showed a linear drug-release pattern with a higher drug release compared with the poorly water-soluble raw Active Pharmaceutical Ingredient (API) (38 ± 3%). Similar rifabutin dissolution profiles were reported from glyceryl dibehenate and glyceryl tristearate solid-lipid nanoparticles (65 and 80% after 1 h, respectively) (Gaspar

Table 2
Physicochemical characterization of blank and rifabutin-loaded (1, 2.5, and 5%) protamine nanocapsules (NCs) after one month of storage as suspension (at 4 °C) or as a freeze-dried powder (RT). Particle size and polydispersity index were obtained by Dynamic Light Scattering. Data represent mean ± SD, $N = 3$.

Conditions	Freeze-dried (RT)			Suspension (4 °C)		
Formulation	Size (nm)	PDI	Charge (mV)	Size (nm)	PDI	Charge (mV)
Blank NCs	222 ± 32	<0.3	12 ± 9	229 ± 52	<0.2	11 ± 9
1% Rifabutin NCs	202 ± 36	<0.3	17 ± 8	229 ± 64	<0.2	9 ± 10
2.5% Rifabutin NCs	199 ± 23	<0.3	13 ± 7	208 ± 30	<0.2	13 ± 11
5% Rifabutin NCs	204 ± 19	<0.3	13 ± 9	213 ± 35	<0.2	13 ± 8

et al., 2016).

Various kinetic models were used to evaluate the drug release pattern of protamine NCs using DDSolver software (Zhang et al., 2010), and the best-fitted models were selected based on the adjusted coefficient of determination R^2, adj R^2, and Akaike Information Criterion (ACI) (Supplementary Table 2). Protamine NCs were found to be a better fit for both the First Order and Korsmeyer-Peppas > Higuchi model, which explains a concentration-dependent drug release (First Order kinetics) but also a diffusion of the drug from the polymeric matrix (Korsmeyer-Peppas). The n value indicated that 1 and 5% rifabutin formulations followed a non-Fickian diffusion of the drug ($n = 0.82$ and 0.94, respectively) while 2.5% followed Fickian drug diffusion ($n = 0.28$), thus observing a change in the sorption process once the equilibrium by the surface concentration of drugs was achieved. (ACI) values confirmed that first-order kinetics gave the best fit out of the set of models. Rifabutin release profile from nanocapsules was similar to that obtained with other previously reported rifabutin-based formulations, supporting that the matrix is responsible of the release pattern: rifabutin release was faster in the case of formulations that used hydrophilic polymers devoid of crosslinking agents, such as low molecular weight chitosan or fucoidan, while it slowed down when viscous solutions as locust bean gum or chitosan with a higher degree of crosslinking were used (Rodrigues et al., 2020).

3.4. *In vitro permeability studies*

The amount of Active Pharmaceutical Ingredient dispersed from the simulated lung media through the epithelium was evaluated by diffusion in a modified side-by-side® model, and the measurements took place in real time. The maximum permeability of rifabutin was about 70 μg/cm^2 after 35 min, not observing a greater increase in permeability and reaching a plateau at this point. However, the diffusion of rifabutin-loaded nanocapsules was slower and more progressive, as shown in Fig. 5, with a linear trend. In the case of 1% and 5% rifabutin-loaded protamine NCs diffusion was apparently faster (90 ± 14 and 78 ± 32 μg/cm^2 after 1 h), while in the case of 2.5% was 57 ± 5 μg/cm^2.

Despite rifabutin is characterized by its high permeability and low solubility (Nighute and Bhise, 2009), stagnation takes place without observing further increase in the permeability after 35 min. The flux (J) and the permeability coefficient (Kp) (Table 3) of the nanocapsules were higher than that of the raw rifabutin for all the formulations except 2.5% rifabutin-loaded protamine NCs. However, a progressive and constant permeability of the drug through the membrane with a linear tendency was observed and the growing trend is expected to exceed the maximum obtained from the raw drug at more extended times.

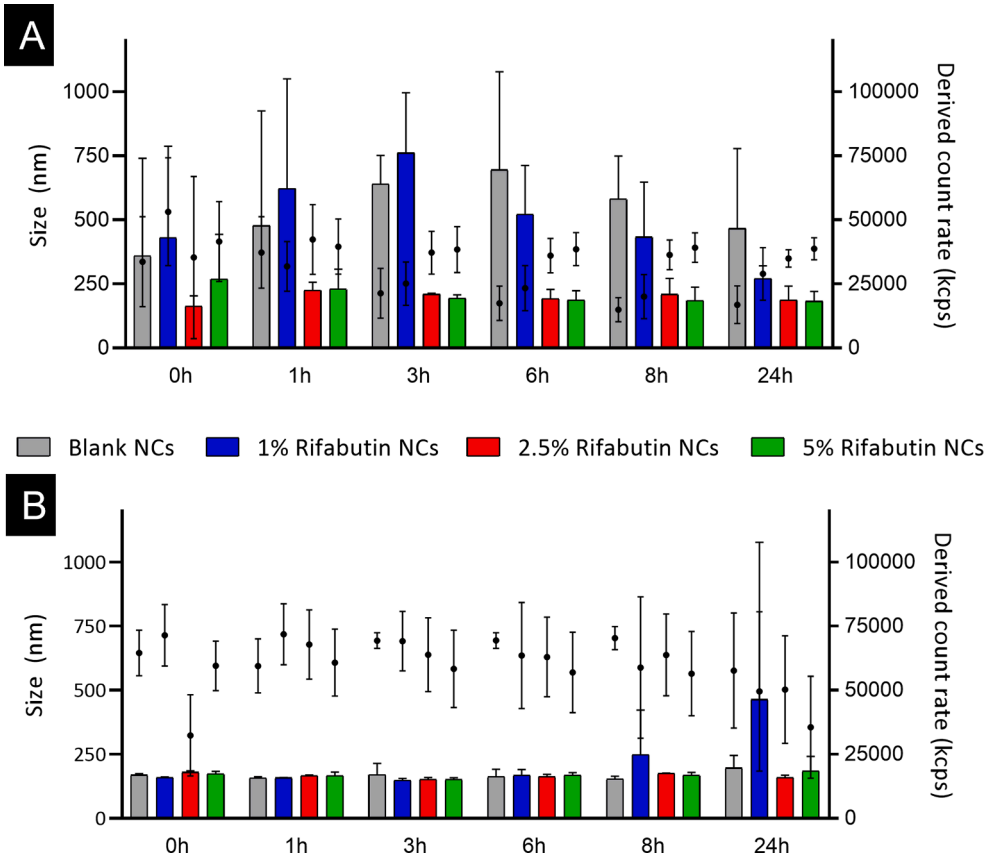

Fig. 3. Stability of rifabutin-loaded protamine nanocapsules (NCs) after incubation in (A) cell culture media DMEM and (B) Simulated Lung Media at 37 °C by Dynamic Light Scattering. Size=Bars, Derived count rate= Dots. Data represent mean ± SD, $N = 5$ independent measurements.

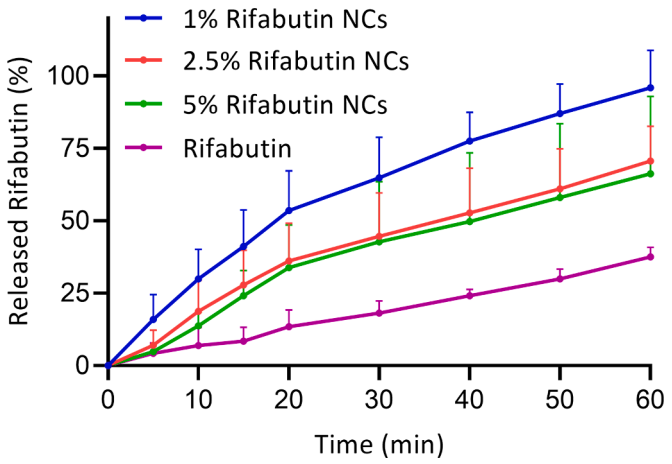

Fig. 4. *In vitro* dissolution results of the drug from the developed 1%, 2.5%, and 5% rifabutin-loaded protamine nanocapsules (NCs). Data represent mean ± SD, $N = 3$ independent measurements.

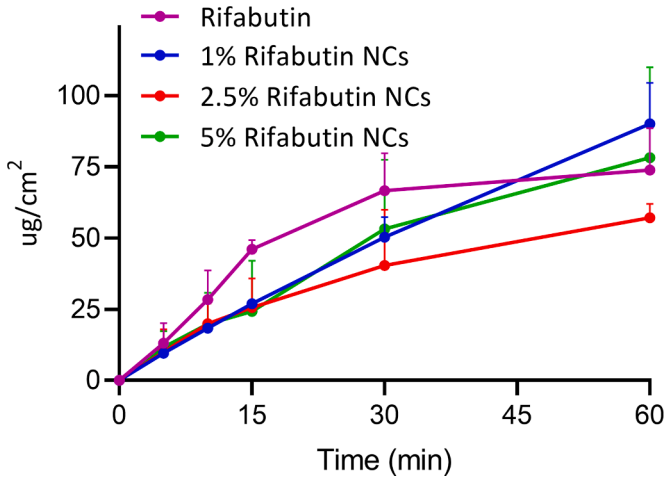

Fig. 5. *In vitro* results of the API (rifabutin) permeability from the developed 1%, 2.5%, and 5% rifabutin-loaded protamine nanocapsules (NCs) compared with the raw drug. Data represent mean ± SD, $N = 3$ independent measurements.

Table 3
In vitro permeability results of the samples. Data represent mean ± SD, $N = 3$ independent measurements.

Formulation	J (μg/cm^2/h)	Kp (cm/h)
free Rifabutin	73.82	0.0984
1% Rifabutin NCs	90.08	0.1201
2.5% Rifabutin NCs	57.07	0.0761
5% Rifabutin NCs	78.15	0.1042

3.5. *In vitro toxicity assays*

An MTT assay was performed to investigate the cytotoxicity of the developed nanocapsules in lung derived A549 cells and Raw 264.7 macrophages. The cell viability was observed to be concentration-dependent (from 0.1 to 1 mg/mL NCs concentrations) after 24 h, as reported in Fig. 6. The rifabutin-loaded NCs showed more than 50% cell viability at 0.25 mg/mL and more than 75% viability at concentrations of 0.1 mg/mL. The toxicity values obtained at high concentrations of nanocapsules may be due to the affinity of cationic nanocarriers towards macrophages, which leads to a greater electrostatic attraction with their negatively charged cell surface (Robla et al., 2021), thus increasing the metabolic activity of macrophages. For all formulations, the toxicity of the encapsulated drug was similar to the reported for free rifabutin (>50% toxicity at 12.5 μg/mL for Raw 264.7 cells and 20 μg/mL for A549 cells, data not shown). 1 mg/mL formulations were equivalent to 10, 25, and 50 μg/mL of encapsulated drug of 1, 2.5, and 5% rifabutin protamine NCs, respectively.

3.6. *Quantitative nanocapsule uptake*

Confocal laser scanning microscopy (CLSM) was performed for the qualitative assessment of the fluorescent-DiD labeled rifabutin-loaded protamine NCs in human alveolar epithelial cells A549 and macrophages Raw 264.7. For this purpose, protamine nanocapsules were initially formulated with the drug as described above, carrying out the incorporation of DiD dye in the oily phase. Its physicochemical properties were characterized by DLS and drug association by UPLC (Supplementary Table 3) showing sizes similar to those previously reported and with a slightly lower association of rifabutin, which could be related to drug-rifabutin competition in the oily nucleus. NCs internalization with a cytoplasmatic distribution was observed in both cell lines (Fig. 7) when compared with control (untreated cells). Bright-field analysis (Supplementary Fig. 2) allows us to delimit the different cells, confirming that an internalization or adsorption of the NCs takes place in the plasma membrane surrounding cell nuclei.

Quantification of the percentage of DiD-labeled rifabutin-loaded NCs uptake was also performed by flow cytometry (Fig. 8). Histograms of the control cells were compared with those of A549 and Raw 264.7 cells treated with 1, 2.5, and 5% rifabutin-loaded protamine NCs. Internalization was found to be of >90% in all cases (93, 95, 98, and 96% of the A549 cells, and 96, 97, 99, and 98% of the Raw 264.7 cells were internalized by blank, 1, 2.5, and 5% rifabutin-loaded protamine NCs, respectively). The internalization of the rifabutin-loaded protamine NCs in the A549 cells after evaluation of the Mean Fluorescence Intensity (MFI) was found to be 8–12 times higher compared with control. Raw 264.7 macrophages showed an MFI 2–3 times higher than untreated cells, for blank, 1%, 2.5 and 5% rifabutin-loaded protamine NCs, respectively. It has been reported that the physicochemical characteristics of nanoparticles influence their mechanism of entry into cells (Lee et al., 2015), thus, the size of the developed nanocapsules could also lead to their internalization through phagocytic and non-phagocytic mechanisms, such as micropinocytosis.

3.7. *IDO assay*

IDO is an immune-suppressive enzyme in macrophages and dendritic cells involved in tryptophan catabolism into kynurenine, which induces Th_1 cell apoptosis *in vitro*. Th_1 are the main effector CD4+ T lymphocytes during TB, contributing to protection against TB by secreting IFN-γ (Lyadova and Panteleev, 2015). As IDO expression can impact peripheral tolerance and immune regulation, we evaluated the tolerogenic response of the rifabutin-loaded protamine NCs by quantifying the IDO enzymatic activity in human monocyte-derived macrophages. We observed that the response was similar for all the formulations compared to non-treated macrophages used as control (Fig. 9), indicating no tolerogenic effect (pro-inflammatory response) of the formulations. Given that macrophages are capable of internalizing rifabutin-loaded protamine NCs, and that Mtb suppresses the antimicrobial response of macrophages (Bekale et al., 2019), the developed systems could be interesting in terms of macrophage immune modulation, being able to activate these immune cells and creating a hostile environment for Mtb.

3.8. *Blood compatibility test*

Although inhaled particles do not come in contact with blood immediately, the high permeability of air-blood barrier of the alveoli

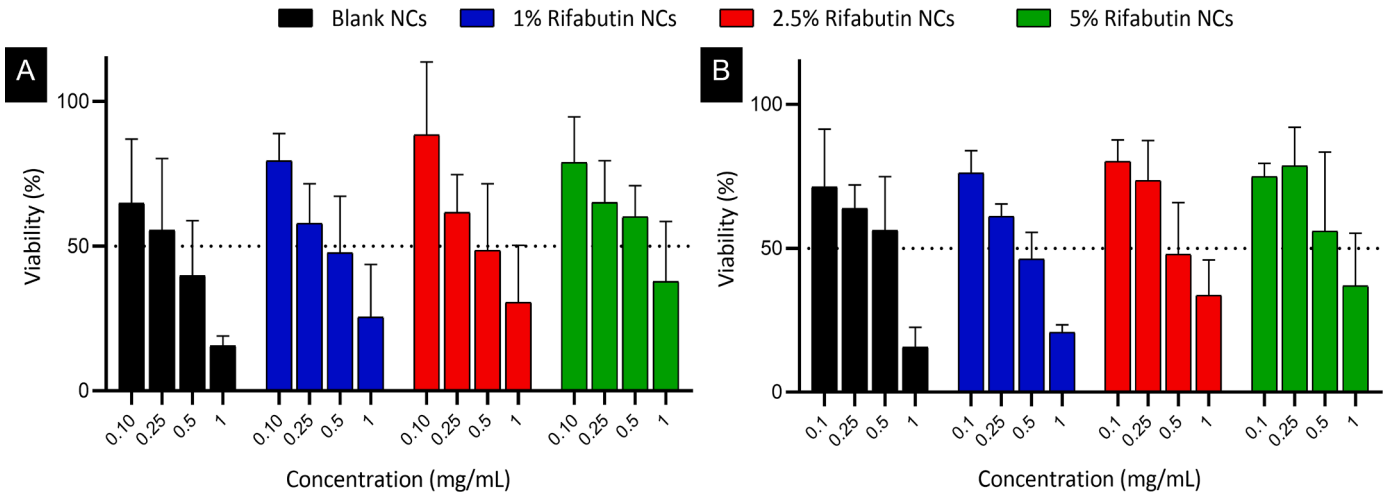

Fig. 6. *In vitro* evaluation of the effect of the developed 1%, 2.5%, and 5% rifabutin-loaded protamine nanocapsules (NCs) on the viability of A549 cells (A) and Raw 264.7 macrophages (B). Data represent mean ± SD, $N = 3$ independent measurements.

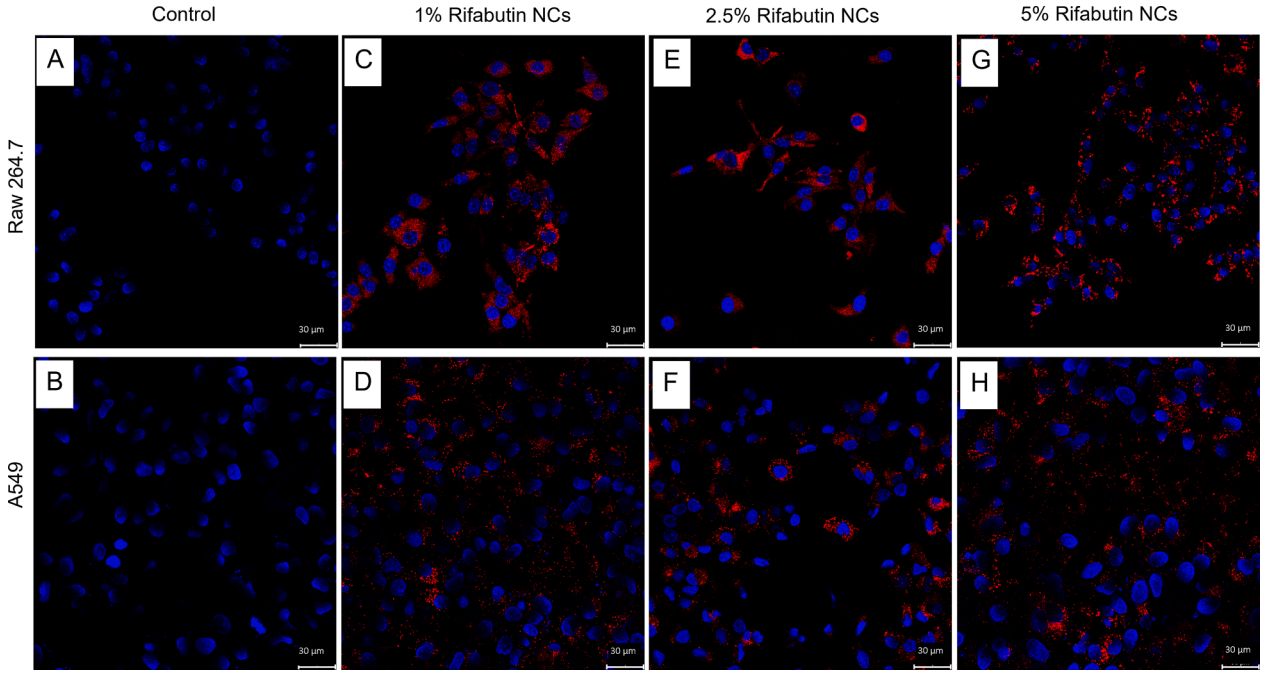

Fig. 7. Cellular internalization study via confocal imaging of Raw 264.7 (A, C, E, and G) and A549 (B, D, F, and G) cell lines. DAPI-dye (blue channel; Excitation λ_{max} = 359 nm, Emission λ_{max} = 457 nm); DiD-dye (red channel; Excitation λ_{max}=640 nm, Emission λ_{max}= 675 nm). The scale bar represents 30 µm.

(with a thickness of 0.1–0.2 µm) allows fast uptake of particles (Fröhlich, 2017). A hemolysis assay was performed to demonstrate nanocarrier biocompatibility with the bloodstream to get insight into the behavior of formulations for *in vivo* applications. As shown in Fig. 10, the rifabutin-loaded nanocapsules posed no toxicity on the RBCs in the concentration range used in this study, indicating their hemocompatibility and the preservation of integrity and functionality of erythrocytes. Although positively charged nanoparticles interact electrostatically with the erythrocyte membrane, which can cause its rupture (Singh et al., 2020), the developed nanocapsules did not influence haemotoxicity. Similar results were also reported for cationic chitosan nanoparticles for the pulmonary delivery of isoniazid (Mukhtar et al., 2022).

3.9. Thermal analysis using DLS

To perform a spray drying process where an increase in the temperature of the formulations is required, it is necessary to previously evaluate its effect on particle size. The low hygroscopic nature of mannitol allows for a low drying temperature for the preparation of dry powder (Munir et al., 2022). Likewise, the use of the Nano Spray Dryer allows outlet temperatures between 28 °C and 59 °C for aqueous solutions. Furthermore, even if a high inlet temperature were used, it has been shown that has minimal impact on particle size during the spray drying process (Arpagaus, 2011). As shown in Fig. 11, the heating process did not induce particle size changes in the developed protamine nanocapsules up to 90 °C, as their size remained unchanged during the whole thermal analysis. Therefore, we can conclude that the developed systems meet the compatibility requirements for their spray-drying and are not expected to suffer degradation under the processing conditions.

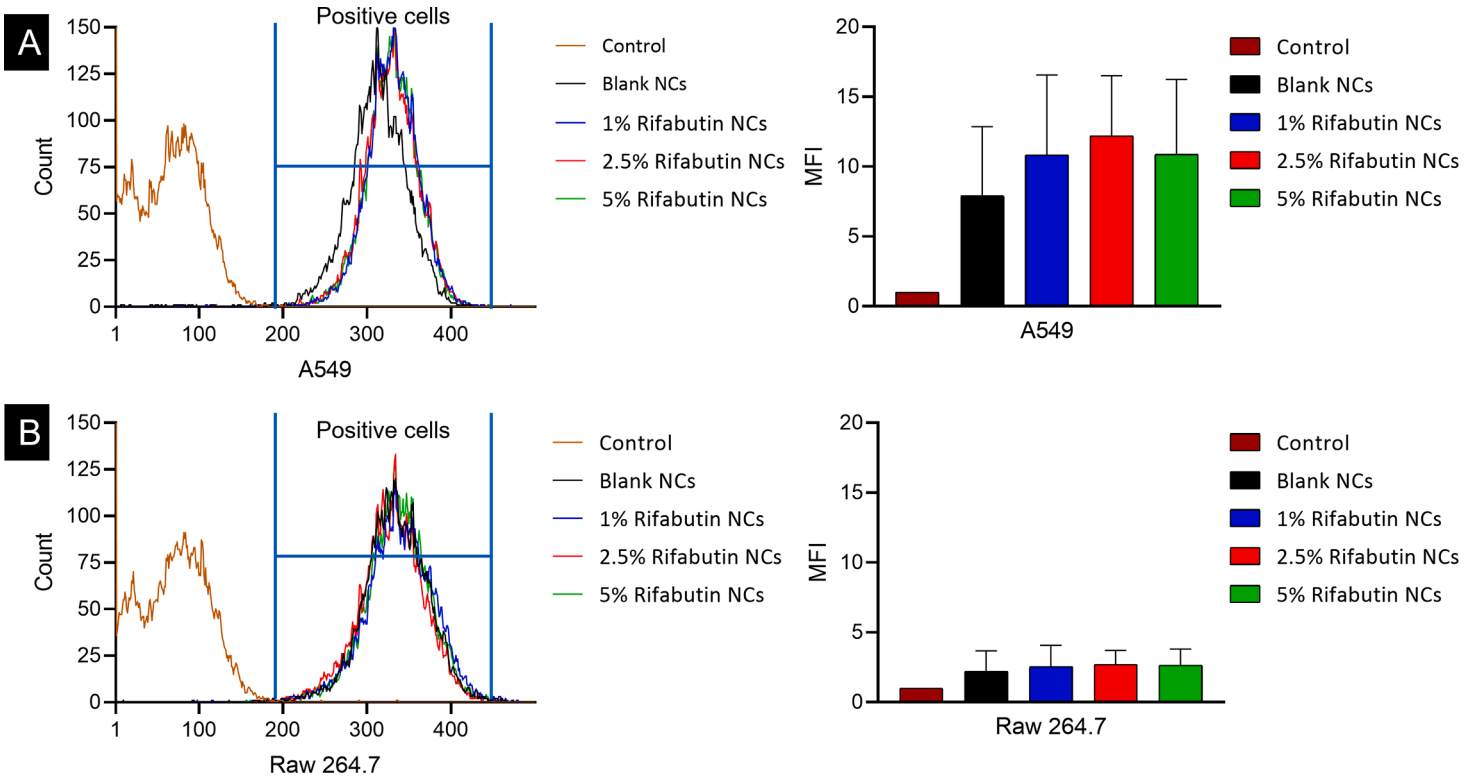

Fig. 8. Flow cytometry histograms and Mean Fluorescent Intensity (MFI) of (A) A549 cells and (B) Raw 264.7 cells after incubation with rifabutin-loaded protamine nanocapsules (NCs). MFI=1 was established for control (non-treated cells).

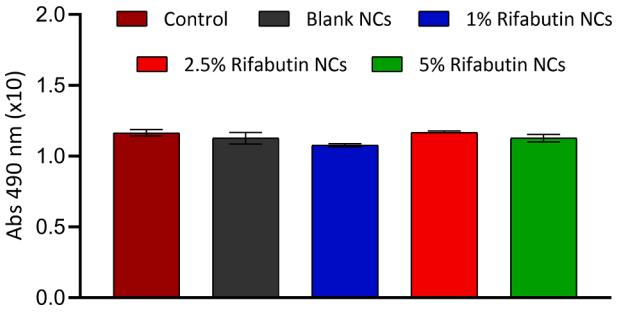

Fig. 9. Indoleamine 2,3-dioxygenase (IDO) activity in human-derived macrophage cultures after incubation with rifabutin-loaded protamine nanocapsules (NCs). Data represents mean ± SEM (Standard Error Mean); $N = 3$ different donors.

3.10. Preparation of pulmonary dry powders containing rifabutin protamine nanocapsules

D-mannitol is a nontoxic and degradable carbohydrate widely used as excipients for dry powder inhalers, approved by the Food and Drug Administration (FDA) (Sham et al., 2004). D-mannitol is a non-reducing and non-hygroscopic compound widely used in aerosolization. During this process, it can give rise to different pure polymorphs (mainly α, β, or δ), with greater kinetic stability than its hydrated and amorphous form (Altay Benetti et al., 2021). Mannitol is approved as a dry powder formulation for the treatment of bacterial infections in cystic fibrosis (Bronchitol®) (Burness and Keating, 2012). Although its effect in TB treatment has not been reported, its high aqueous solubility and osmolarity properties make it an interesting candidate to overcome the mucus absorption barrier, reaching alveoli tuberculosis-infected macrophages. The 80/20 (mannitol/nanocapsules) ratio used and the solid content was established according to previous studies with mannitol that showed that 20% (w/w) of nanoparticles allowed the obtaining of dry non-aggregated powders with desirable droplet size (Al-Qadi et al., 2012; Grenha et al., 2005). It was also considered because as Miglyol® is a lipid with a low melting point, higher excipient amounts were required to protect it from high temperatures during the spray-drying process, as also reported for lipids such as glyceryl dibehenate and glyceryl tristearate (Gaspar et al., 2017). The rifabutin-loaded protamine NCs were co-spray dried with D-mannitol (Section 2.12) and then characterized using DSC, Andersen Cascade Impactor, and Aerosizer® LD.

As reported in DSC thermograms (Fig. 12A), the spray-dried nanoparticles exhibited a sharp peak at 165 °C (endothermic peak) due to the presence of D-mannitol in the spray-drying process. The presence of a melting peak at 155 °C followed by an exothermic recrystallization peak at about 157 °C and a final melting around 165 °C is attributable to a change from a mixture of α-β D-mannitol forms to a δ polymorph (Altay Benetti et al., 2021). The disappearance of the peak for the pure drug, which shows a melting endotherm at approximately 149 °C (Gaspar et al., 2016), could be attributed to its encapsulation inside the developed spray-dried NCs (Chokshi et al., 2018). XRPD pattern (Fig. 12B) confirmed the crystalline structure of the spray-dried formulation and showed an intense peak at 9.7° 2-theta which is typical of δ-form mannitol (Kwok et al., 2015). δ-mannitol polymorph has been described as having better compaction behavior, tabletability, and friability compared to α- and β-mannitol (De Pauw et al., 2022; Vanhoorne et al., 2016). Rifabutin peaks at 10.75, 12.63, 15.50, 17.9, 18.9, and 22.8 2-theta are indicative of its crystalline state (Shanmuga Priya et al., 2013). The XRPD pattern of the spray-dried rifabutin-loaded NCs also manifests the effective inclusion of the drug in the system as groups responsible for the crystallinity of rifabutin are included in the spray-dried formulations.

3.11. In vitro drug deposition evaluation

Andersen Cascade Impactor evaluation was performed for the aerodynamic evaluation of the spray-dried powders and the distribution of the SPD nanocapsules was determined during the aerodynamic

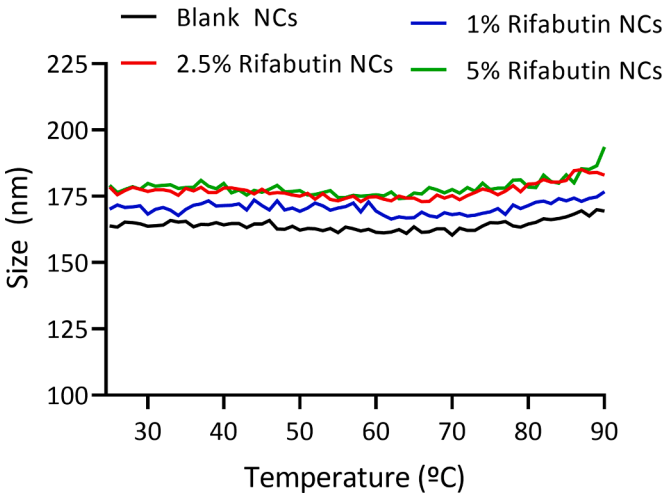

Fig. 11. DLS thermograms blank, 1, 2.5, and 5% rifabutin-loaded protamine nanocapsules (NCs) from 25 °C to 90 °C. Results are expressed as mean, $N = 3$. SD values were <10%.

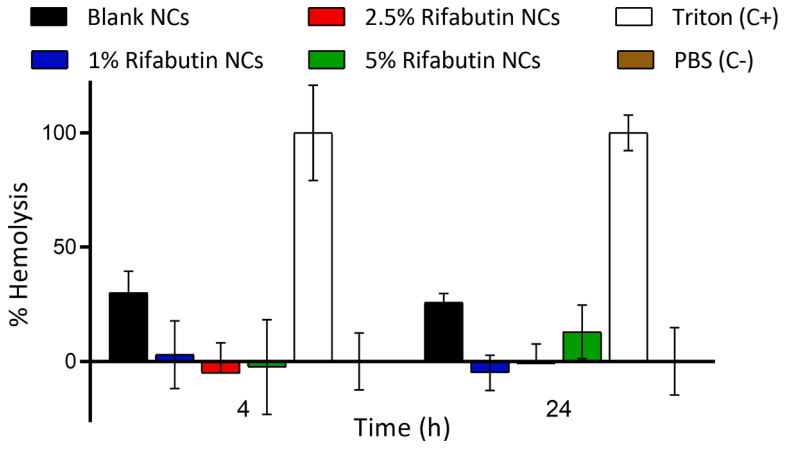

Fig. 10. *In vitro* hemolysis assay after 4 and 24 h was performed on fresh human blood obtained from donors after consent. NCs: Nanocapsules, C+: Positive control, C-: Negative control. Results are expressed as mean ± SEM (Standard Error Mean), $N = 3$ different donors.

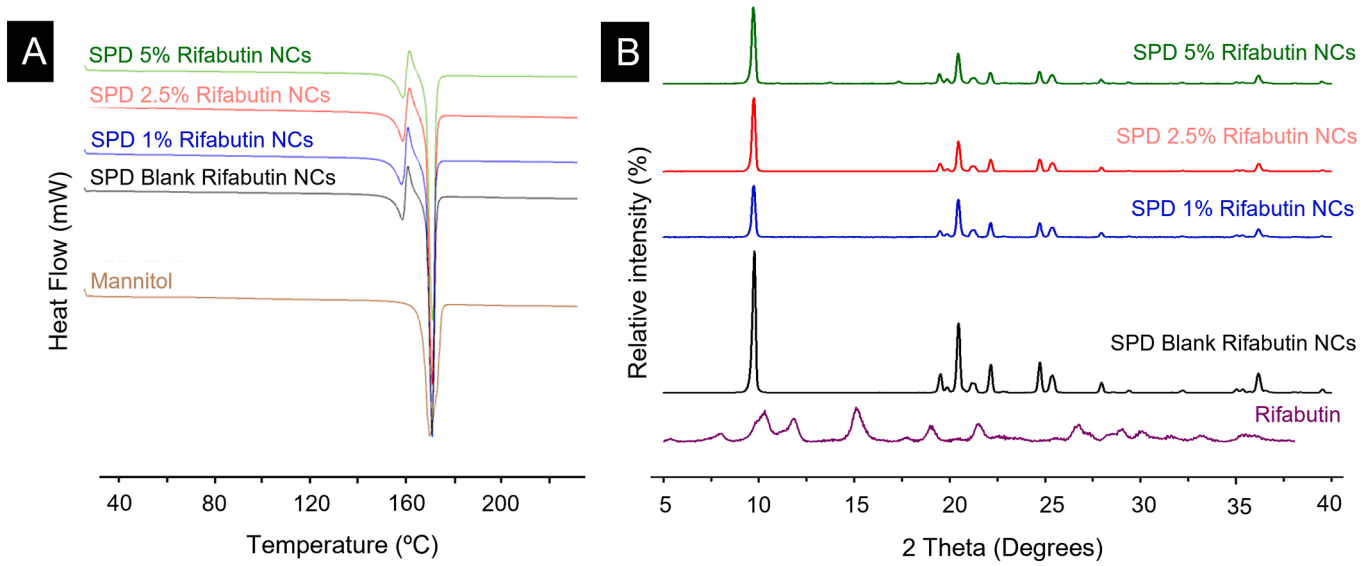

Fig. 12. (A) DSC thermograms and (B) XRPD diffractograms of the raw materials and the spray-dried (SPD) blank and 1, 2.5, and 5% rifabutin-loaded nanocapsules (NCs).

Table 4
In vitro aerodynamic properties of the mannitol spray-dried (SPD) powders at a ratio of 80/20. FPD: Fine Particle Dose; FPF: Fine Particle Fraction (<5 μm); ED: Emitted Dose; MMAD: Mean Medium Aerodynamic Diameter. Data represent mean ± SD, $N = 3$ independent measurements.

Spray-dried powder	Andersen Cascade Impactor				Dynamic Light Scattering		
	FPF (%)	FPD (mg)	ED (%)	MMAD (μm)	Size (nm)	PDI	Charge (mV)
SPD Blank NCs	32 ± 10	1.8 ± 1	77 ± 8	4.2 ± 0.8	290 ± 34	<0.4	19 ± 6
SPD 1% Rifabutin NCs	26 ± 6	1.1 ± 0.4	75 ± 11	5.8 ± 1.4	259 ± 32	<0.3	18 ± 7
SPD 2.5% Rifabutin NCs	19 ± 8	0.8 ± 0.6	69 ± 25	5.8 ± 1.3	564 ± 104	<0.6	19 ± 2
SPD 5% Rifabutin NCs	26 ± 8	1.2 ± 0.6	80 ± 9	5.5 ± 1.8	487 ± 96	<0.7	14 ± 3

assessment. The *in vitro* aerodynamic results calculated by the Inhalytix™ software are presented in Table 4, and the ED, FPF, FPD, and MMAD obtained indicated the DPI performance. The ED percentages were remarkably high for all the formulations as were obtained in the range of 69–80%. The co-spray-dried powders exhibited appropriate aerosolization properties with an FPF of 19 to 32%, indicative of the proportion of the dose delivered to the smaller airways (<5 μm). Similar FPF values for the low-resistance inhaler have been reported for the Breezhaler® device, which was selected because of its suitability for use in patients with a range of disease severities (Chapman et al., 2011). The breathing parameters affect DPI airway deposition for this device, as shown for commercialized Onbreez Breezhaler®, which presented sensitive changes of FPF, with values no higher than 36% for 90 L/min (r^2=0.81) (Horváth et al., 2020). MMADs ranged from 4.2 to 5.8 μm and were optimal for depositing in the bronchi and alveoli (Carvalho et al., 2011). Spray-dried NCs redispersion and size analysis confirmed the stability of colloidal systems during the drying process, as all formulations were kept on the nano-range size fulfilling our aim. However, an

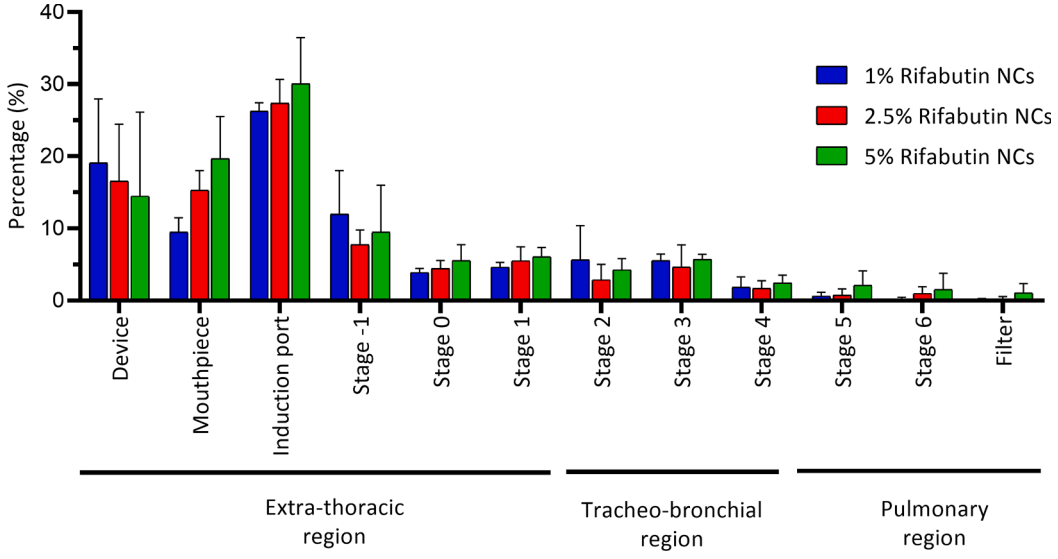

Fig. 13. *In vitro* aerodynamic deposition of spray-dried, rifabutin-loaded protamine nanocapsules (NCs) in the Andersen cascade impactor. Values represent mean ±SD, $N = 3$ independent measurements.

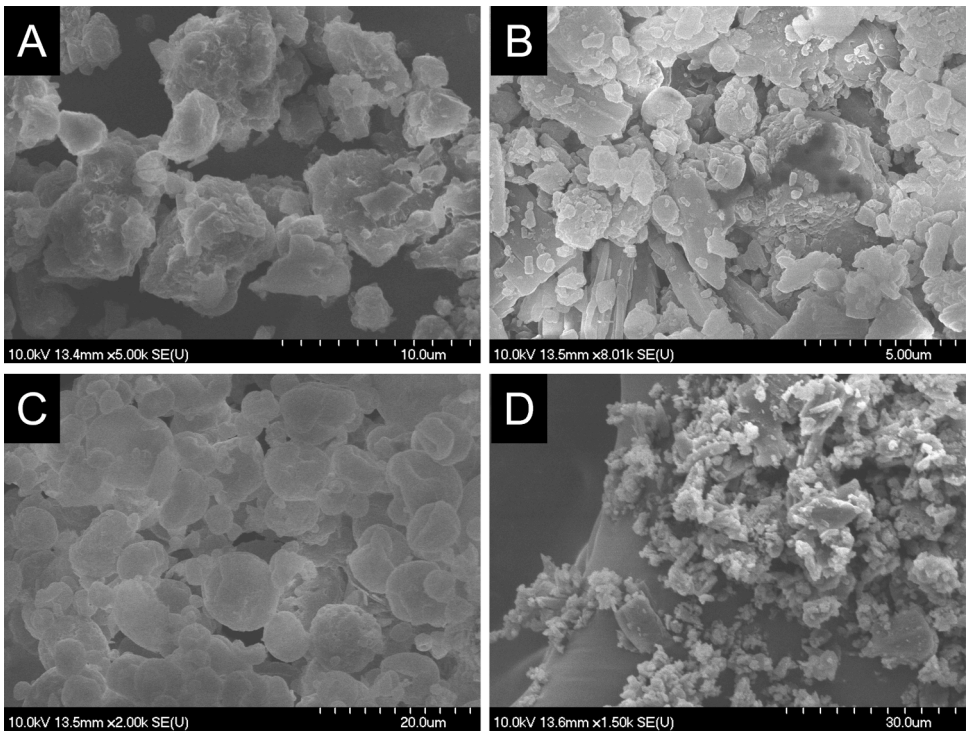

Fig. 14. Electron microscopy scanning images of blank (A), 1% (B), 2.5% (C), and 5% (D) rifabutin-loaded protamine nanocapsules (NCs) after mannitol spray-drying process.

increase of 2.8 and 2.3-fold was observed in the reconstituted 2.5 and 5% rifabutin-loaded NCs compared to the nanocapsules before the spray-dried process. These changes in size were also reported in the development of mannitol spray-dried rifabutin-loaded solid-lipid nanoparticles (Gaspar et al., 2017).

Fig. 13 illustrates the stage-by-stage deposition profiles of spray-dried rifabutin NCs in the ACI after aerosolization. The use of mannitol improved the aerosolization of the nanocapsules as they were successfully released from the capsule in large amounts. Spray-dried rifabutin NCs were distributed mainly through the extra-thoracic region (63–79% of the total amount), especially on the trachea (25–30%). However, the spray-dried powders reached the fourth stage (15–18%), which corresponds to the bronchial area, as well as the alveolar region (1–9% of the total amount).

Particle size distributions were confirmed by the time-of-flight measurements using an Aerosizer LD (Supplementary Fig. 3). For all the samples, similar aerodynamic size distributions were obtained for the whole set of experimental conditions with an average diameter of 2.9 ± 1.9, 2.5 ± 2, 2.3 ± 1.9 and 2.4 ± 1.8 μm with specific surface areas of 0.62, 0.48, 0.67 and 0.84 m^2/g for blank, 1, 2.5 and 5% rifabutin protamine NCs, respectively. The slight decrease in size when using this technique compared to the ACI analysis may be due to the use of maximum shear pressure (Adi et al., 2006) which can cause a slight particle breakage (Bennett et al., 2011). However, this shear is recommended for the analysis of size powders (<20 μm), being of 3 PSI with normal deagglomeration and a medium feed rate of 5000 cts/sec. Microscopy evaluation was performed to support the quantitative evaluation, and the size distribution was corroborated by SEM photomicrographs (Fig. 14), where the rifabutin spray-dried NCs presented mainly a spherical shape with a homogeneous distribution, and we could observe the nanosized active ingredient particles. The diameter of the spray-dried NCs was measured with the Image-J program. The size range obtained was between 4.1 and 5.1 μm and was correlated with the results of the aerodynamic characterization.

The inspiratory flow generated by the patient and the specific resistance of the device are the two driving forces affecting DPIs. In the case of Breezhaler®, a low air-resistance device, its low specific intrinsic resistance (R_D) of 0.060 (cm $H_2O)^{0.5}$ [L/min] $^{-1}$ requires a lower inhalation effort (30 L/min or below), allowing for a greater flow rate. Breezhaler® PIF (peak inspiratory flow rate) is achieved at 108 L/min and requires an inspiratory effort (ΔP) in the of about 4 kPa, lower than Diskus®, Turbuhaler® or Handihaler® (Altman et al., 2018; Dal Negro, 2015; Molimard et al., 2021). Tuberculosis results in impaired lung function, in the form of obstructive lung disease or through reduced lung function, factors that may influence the reduction in PIF (Chushkin and Ots, 2017). Therefore, a flow of 60 L/min was established according to previous works in the field (Gaspar et al., 2017; Grenha et al., 2020; Mukhtar et al., 2021) Considering a flow rate of 60 L/min, 4 s was established as time to achieve the normal forced inhalation volume of an average sized male (4 L) (Momin et al., 2019). Following the equation $\Delta P^{1/2} = R_D Q$ (Tee et al., 2000), the inspiratory effort (drop pressure) generated at 60 L/min was found to be of 1.44 kPa, which could underestimate the real performance of the Breezhaler®, comparing with drop pressure at PIF, which assures an optimal drug delivery to distal airways. This could explain the emitted dose achieved, as small amounts of the DPI were left in the capsule after the first inhalation. This could be improved with repetated inhalations to ensure full dose delivery.

Finally, to provide a higher concentration in the extrapulmonary region, doses between 10 and 100 mg of drug are estimated as necessary in the treatment of tuberculosis, which is less than the conventional oral/parenteral dose of the drug (Momin et al., 2018). Spray-drying technique produces voluminous powders, limiting the amount in a single dose capsule. In this case, the use of 4 capsules (type 3 hard gelatin) would allow to fill of around 1.82 g of powder (1.52 g/mL Aerosizer®, data not shown), equivalent to 30 mg of drug for 5% rifabutin protamine nanocapsules. However, it is to be highlighted that drug activity in alveolar macrophages would be required to establish the necessary dose of rifabutin, which we estimate to be far below the theoretically calculated value.

4. Conclusions

In this study, the developed rifabutin-loaded protamine nanocapsules presented a high encapsulation rate of the drug and have shown promising results on the improvement of dissolution and permeability of the drug. The developed formulation is well tolerated by alveolar macrophages and has a strong capacity to be internalized and activate them. Furthermore, rifabutin-loaded protamine nanoparticles could be successfully incorporated in microparticles by co-spray drying with mannitol for the obtention of a dry powder with adequate aerodynamic properties. The developed ready-to-use pulmonary dry powder system holds great promise for inhalable therapy of pulmonary tuberculosis. Future studies will be required to evaluate the antibacterial efficacy of the systems developed after *in vivo* pulmonary administration.

Ethics approval

Informed consent was obtained from all subjects involved in the study. All the procedures were carried out under the ethical standard of the institute and national committee on human experiments and the Declaration of Helsinki. Permission was acquired from the Institutional Ethics Committee (Comité Ético de Investigación Clínica de Galicia, CEIC), approval number 2014/543.

CRediT authorship contribution statement

Sandra Robla: Formal analysis, Investigation, Methodology, Software, Visualization, Writing – original draft, Writing – review & editing. **Rubén Varela Calviño:** Supervision, Writing – review & editing. **Rita Ambrus:** Conceptualization, Funding acquisition, Resources, Supervision, Validation, Visualization, Writing – review & editing. **Noemi Csaba:** Conceptualization, Funding acquisition, Resources, Project administration, Supervision, Validation, Visualization, Writing – review & editing.

Declaration of Competing Interest

The authors declare no conflict of interest.

Data availability

Data will be made available on request.

Acknowledgments

This research was funded by Ministerio de Ciencia e Innovacion RETOS - PID2019-107500RB-I00, Ministry of Human Capacities, Hungary grant TKP2021-EGA-32 and the Erasmus+ program of the European Union.

Supplementary materials

Supplementary material associated with this article can be found, in the online version, at doi:10.1016/j.ejps.2023.106442.

References

Adi, H., Larson, I., Chiou, H., Young, P., Traini, D., Stewart, P., 2006. Agglomerate strength and dispersion of salmeterol xinafoate from powder mixtures for inhalation. Pharm. Res. 23, 2556–2565. https://doi.org/10.1007/s11095-006-9082-6.

Al-Qadi, S., Grenha, A., Carrión-Recio, D., Seijo, B., Remuñán-López, C., 2012. Microencapsulated chitosan nanoparticles for pulmonary protein delivery: *in vivo* evaluation of insulin-loaded formulations. J. Control. Release 157, 383–390. https://doi.org/10.1016/j.jconrel.2011.08.008.

Altay Benetti, A., Bianchera, A., Buttini, F., Bertocchi, L., Bettini, R., 2021. Mannitol polymorphs as carrier in DPIs formulations: isolation characterization and performance. Pharmaceutics 13, 1113. https://doi.org/10.3390/pharmaceutics13081113.

Altman, P., Wehbe, L., Dederichs, J., Guerin, T., Ament, B., Moronta, M.C., Pino, A.V., Goyal, P., 2018. Comparison of peak inspiratory flow rate via the Breezhaler®, Ellipta® and HandiHaler® dry powder inhalers in patients with moderate to very severe COPD: A randomized cross-over trial. BMC Pulm. Med. 18, 1–8. https://doi.org/10.1186/s12890-018-0662-0.

Aristoff, P.A., Garcia, G.A., Kirchhoff, P.D., Hollis Showalter, H.D., 2010. Rifamycins – obstacles and opportunities. Tuberculosis 90, 94–118. https://doi.org/10.1016/j.tube.2010.02.001.

Arpagaus, C., 2011. Nano spray dryer B-90: literature review and applications. Büchi Inf. Bull. 8.

Awotwe-Otoo, D., Agarabi, C., Keire, D., Lee, S., Raw, A., Yu, L., Habib, M.J., Khan, M.A., Shah, R.B., 2012. Physicochemical characterization of complex drug substances: evaluation of structural similarities and differences of protamine sulfate from various sources. AAPS J. 14, 619–626. https://doi.org/10.1208/s12248-012-9375-0.

Barreneche, C., Gil, A., Sheth, F., Inés Fernández, A., Cabeza, L.F., 2013. Effect of d-mannitol polymorphism in its thermal energy storage capacity when it is used as PCM. Sol. Energy 94, 344–351. https://doi.org/10.1016/j.solener.2013.05.023.

Bekale, R.B., Du Plessis, S.M., Hsu, N.J., Sharma, J.R., Sampson, S.L., Jacobs, M., Meyer, M., Morse, G.D., Dube, A., 2019. Mycobacterium tuberculosis and interactions with the host immune system: opportunities for nanoparticle based immunotherapeutics and vaccines. Pharm. Res. 36 https://doi.org/10.1007/s11095-018-2528-9.

Benbow, N.L., Rozenberga, L., McQuillan, A.J., Krasowska, M., Beattie, D.A., 2021. ATR FTIR study of the interaction of tio2 nanoparticle films with β-Lactoglobulin and bile salts. Langmuir 37, 13278–13290. https://doi.org/10.1021/acs.langmuir.1c01830.

Bennett, M., Christie, S.M., Graham, A., Thomas, B.S., Vishnyakov, V., Morris, K., Peters, D.M., Jones, R., Ansell, C., 2011. Composition of smoke generated by landing aircraft. Environ. Sci. Technol. 45, 3533–3538. https://doi.org/10.1021/es1027585.

Braunstein, M., Hickey, A.J., Ekins, S., 2019. Why wait? The case for treating tuberculosis with inhaled drugs. Pharm. Res. 36, 166. https://doi.org/10.1007/s11095-019-2704-6.

Burness, C.B., Keating, G.M., 2012. Mannitol dry powder for inhalation: in patients with cystic fibrosis. Drugs 72, 1411–1421. https://doi.org/10.2165/11208950-000000000-00000.

Carvalho, T.C., Peters, J.I., Williams III, R.O., 2011. Influence of particle size on regional lung deposition – What evidence is there? Int. J. Pharm. 406, 1–10. https://doi.org/10.1016/j.ijpharm.2010.12.040.

Chae, J., Choi, Y., Tanaka, M., Choi, J., 2021. Inhalable nanoparticles delivery targeting alveolar macrophages for the treatment of pulmonary tuberculosis. J. Biosci. Bioeng. 132, 543–551. https://doi.org/10.1016/j.jbiosc.2021.08.009.

Chapman, K.R., Fogarty, C.M., Peckitt, C., Lassen, C., Jadayel, D., Dederichs, J., Dalvi, M., Kramer, B., 2011. Delivery characteristics and patients' handling of two single-dose dry-powder inhalers used in COPD. Int. J. Chron. Obstr. Pulm. Dis. 6, 353–363. https://doi.org/10.2147/COPD.S18529.

Chokshi, N.V., Khatri, H.N., Patel, M.M., 2018. Formulation, optimization, and characterization of rifampicin-loaded solid lipid nanoparticles for the treatment of tuberculosis. Drug Dev. Ind. Pharm. 44, 1975–1989. https://doi.org/10.1080/03639045.2018.1506472.

Chushkin, M.I., Ots, O.N., 2017. Impaired pulmonary function after treatment for tuberculosis: the end of the disease? J. Bras. Pneumol. 43, 38–43. https://doi.org/10.1590/s1806-37562016000000053.

Dal Negro, R.W., 2015. Dry powder inhalers and the right things to remember: a concept review. Multidiscip. Respir. Med. 10, 2–5. https://doi.org/10.1186/s40248-015-0012-5.

Davies, G.R., Cerri, S., Richeldi, L., 2007. Rifabutin for treating pulmonary tuberculosis. Cochrane Database Syst. Rev. https://doi.org/10.1002/14651858.CD005159.pub2.

De Pauw, E., Vervaet, C., Vanhoorne, V., 2022. Formation of delta-mannitol by co-spray drying: enhancing the tabletability of paracetamol/mannitol formulations. J. Drug Deliv. Sci. Technol. 77, 103907 https://doi.org/10.1016/j.jddst.2022.103907.

El-Sherbiny, I.M., El-Baz, N.M., Yacoub, M.H., 2015. Inhaled nano- and microparticles for drug delivery. Glob. Cardiol. Sci. Pract. 2 https://doi.org/10.5339/gcsp.2015.2, 2015.

Fröhlich, E., 2017. Hemocompatibility of inhaled environmental nanoparticles: potential use of *in vitro* testing. J. Hazard. Mater. 336, 158–167. https://doi.org/10.1016/j.jhazmat.2017.04.041.

Gaspar, D.P., Faria, V., Gonçalves, L.M.D., Taboada, P., Remuñán-López, C., Almeida, A. J., 2016. Rifabutin-loaded solid lipid nanoparticles for inhaled antitubercular therapy: physicochemical and *in vitro* studies. Int. J. Pharm. 497, 199–209. https://doi.org/10.1016/j.ijpharm.2015.11.050.

Gaspar, D.P., Gaspar, M.M., Eleutério, C.V., Grenha, A., Blanco, M., Gonçalves, L.M.D., Taboada, P., Almeida, A.J., Remuñán-López, C., 2017. Microencapsulated Solid Lipid nanoparticles as a hybrid platform for pulmonary antibiotic delivery. Mol. Pharm. 14, 2977–2990. https://doi.org/10.1021/acs.molpharmaceut.7b00169.

Gaspar, M.M., Cruz, A., Penha, A.F., Reymão, J., Sousa, A.C., Eleutério, C.V., Domingues, S.A., Fraga, A.G., Filho, A.L., Cruz, M.E.M., Pedrosa, J., 2008. Rifabutin encapsulated in liposomes exhibits increased therapeutic activity in a model of disseminated tuberculosis. Int. J. Antimicrob. Agents 31, 37–45. https://doi.org/10.1016/j.ijantimicag.2007.08.008.

Gaspar, M.M., Neves, S., Portaels, F., Pedrosa, J., Silva, M.T., Cruz, M.E.M., 2000. Therapeutic efficacy of liposomal rifabutin in a mycobacterium avium model of infection. Antimicrob. Agents Chemother. 44, 2424–2430. https://doi.org/10.1128/AAC.44.9.2424-2430.2000.

Gieszinger, P., Kiss, T., Szabó-Révész, P., Ambrus, R., 2021. The development of an *in vitro* horizontal diffusion cell to monitor nasal powder penetration inline. Pharmaceutics 13, 809. https://doi.org/10.3390/pharmaceutics13060809.

Grenha, A., Alves, A.D., Guerreiro, F., Pinho, J., Simões, S., Almeida, A.J., Gaspar, M.M., 2020. Inhalable locust bean gum microparticles co-associating isoniazid and rifabutin: Therapeutic assessment in a murine model of tuberculosis infection. Eur. J. Pharm. Biopharm. 147, 38–44. https://doi.org/10.1016/j.ejpb.2019.11.009.

Grenha, A., Seijo, B., Remuñán-López, C., 2005. Microencapsulated chitosan nanoparticles for lung protein delivery. Eur. J. Pharm. Sci. 25, 427–437. https://doi.org/10.1016/j.ejps.2005.04.009.

Grenha, A., Seijo, B., Serra, C., Remuñán-López, C., 2007. Chitosan nanoparticle-loaded mannitol microspheres: structure and surface characterization. Biomacromolecules 8, 2072–2079. https://doi.org/10.1021/bm061131g.

Horváth, A., Farkas, Á., Szipőcs, A., Tomisa, G., Szalai, Z., Gálffy, G., 2020. Numerical simulation of the effect of inhalation parameters, gender, age and disease severity on the lung deposition of dry powder aerosol drugs emitted by Turbuhaler®, Breezhaler® and Genuair® in COPD patients. Eur. J. Pharm. Sci. 154 https://doi.org/10.1016/j.ejps.2020.105508.

Jakubiak, P., Thwala, L.N., Cadete, A., Préat, V., Alonso, M.J., Beloqui, A., Csaba, N., 2017. Solvent-free protamine nanocapsules as carriers for mucosal delivery of therapeutics. Eur. Polym. J. 93, 695–705. https://doi.org/10.1016/j.eurpolymj.2017.03.049.

Kastury, F., Smith, E., Juhasz, A.L., 2017. A critical review of approaches and limitations of inhalation bioavailability and bioaccessibility of metal(loid)s from ambient particulate matter or dust. Sci. Total Environ. 574, 1054–1074. https://doi.org/10.1016/j.scitotenv.2016.09.056.

Khairuddin, Pramono, E., Utomo, S.B., Wulandari, V., Zahrotul W, A., Clegg, F., 2016. FTIR studies on the effect of concentration of polyethylene glycol on polimerization of Shellac. J. Phys. Conf. Ser. 776, 012053 https://doi.org/10.1088/1742-6596/776/1/012053.

Kwok, P.C.L., Grabarek, A., Chow, M.Y.T., Lan, Y., Li, J.C.W., Casettari, L., Mason, A.J., Lam, J.K.W., 2015. Inhalable spray-dried formulation of D-LAK antimicrobial peptides targeting tuberculosis. Int. J. Pharm. 491, 367–374. https://doi.org/10.1016/j.ijpharm.2015.07.001.

Lado, F.L.L., 2002. Clínica de la tuberculosis 39, 181–192.

Lee, W.H., Loo, C.Y., Traini, D., Young, P.M., 2015. Nano- and micro-based inhaled drug delivery systems for targeting alveolar macrophages. Expert Opin. Drug Deliv. 12, 1009–1026. https://doi.org/10.1517/17425247.2015.1039509.

Lyadova, I.V., Panteleev, A.V., 2015. Th1 and Th17 cells in tuberculosis: protection, pathology, and biomarkers. Mediat. Inflamm. 2015, 1–13. https://doi.org/10.1155/2015/854507.

Malamatari, M., Charisi, A., Malamataris, S., Kachrimanis, K., Nikolakakis, I., 2020. Spray drying for the preparation of nanoparticle-based drug formulations as dry powders for inhalation. Processes 8. https://doi.org/10.3390/pr8070788.

Molimard, M., Kottakis, I., Jauernig, J., Lederhilger, S., Nikolaev, I., 2021. Performance characteristics of breezhaler® and aerolizer® in the real-world setting. Clin. Drug Investig. 41, 415–424. https://doi.org/10.1007/s40261-021-01021-w.

Momin, M.A.M., Rangnekar, B., Sinha, S., Cheung, C.Y., Cook, G.M., Das, S.C., 2019. Inhalable dry powder of bedaquiline for pulmonary tuberculosis: *in vitro* physicochemical characterization, antimicrobial activity and safety studies. Pharmaceutics 11. https://doi.org/10.3390/pharmaceutics11100502.

Momin, M.A.M., Tucker, I.G., Das, S.C., 2018. High dose dry powder inhalers to overcome the challenges of tuberculosis treatment. Int. J. Pharm. 550, 398–417. https://doi.org/10.1016/j.ijpharm.2018.08.061.

Mukhtar, M., Csaba, N., Robla, S., Varela-Calviño, R., Nagy, A., Burian, K., Kókai, D., Ambrus, R., 2022. Dry powder comprised of isoniazid-loaded nanoparticles of hyaluronic acid in conjugation with mannose-anchored chitosan for macrophage-targeted pulmonary administration in tuberculosis. Pharmaceutics 14, 1543. https://doi.org/10.3390/pharmaceutics14081543.

Mukhtar, M., Szakonyi, Z., Farkas, Á., Burian, K., Kókai, D., Ambrus, R., 2021. Freeze-dried vs spray-dried nanoplex DPIs based on chitosan and its derivatives conjugated with hyaluronic acid for tuberculosis: *in vitro* aerodynamic and in silico deposition profiles. Eur. Polym. J. 160 https://doi.org/10.1016/j.eurpolymj.2021.110775.

Munir, M., Kett, V.L., Dunne, N.J., McCarthy, H.O., 2022. Development of a spray-dried formulation of peptide-DNA nanoparticles into a dry powder for pulmonary delivery using factorial design. Pharm. Res. 39, 1215–1232. https://doi.org/10.1007/s11095-022-03256-4.

Nainwal, N., Sharma, Y., Jakhmola, V., 2022. Dry powder inhalers of antitubercular drugs. Tuberculosis 135, 102228. https://doi.org/10.1016/j.tube.2022.102228.

Nighute, A.B., Bhise, S.B., 2009. Enhancement of dissolution rate of rifabutin by preparation of microcrystals using solvent change method. Int. J. PharmTech Res. 1, 142–148.

Nimje, N., Agarwal, A., Saraogi, G.K., Lariya, N., Rai, G., Agrawal, H., Agrawal, G.P., 2009. Mannosylated nanoparticulate carriers of rifabutin for alveolar targeting. J. Drug Target. 17, 777–787. https://doi.org/10.3109/10611860903115308.

Nirbhavane, P., Vemuri, N., Kumar, N., Khuller, G.K., 2017. Lipid nanocarrier-mediated drug delivery system to enhance the oral bioavailability of rifabutin. AAPS PharmSciTech 18, 829–837. https://doi.org/10.1208/s12249-016-0559-2.

Parlati, C., 2008. Respirable microparticles of aminoglycoside antibiotics for pulmonary administration. Dipatamento Farm. PhD, 161.

Robla, S., Prasanna, M., Varela-Calviño, R., Grandjean, C., Csaba, N., 2021. A chitosan-based nanosystem as pneumococcal vaccine delivery platform. Drug Deliv. Transl. Res. 11, 581–597. https://doi.org/10.1007/s13346-021-00928-3.

Rodrigues, S., da Costa, A.M.R., Flórez-Fernández, N., Torres, M.D., Faleiro, M.L., Buttini, F., Grenha, A., 2020. Inhalable spray-dried chondroitin sulphate microparticles: Effect of different solvents on particle properties and drug activity. Polymers 12, 1–13. https://doi.org/10.3390/polym12020425 (Basel).

Rouco, H., Diaz-Rodriguez, P., Gaspar, D.P., Gonçalves, L.M.D., Cuerva, M., Remuñán-López, C., Almeida, A.J., Landin, M., 2020. Rifabutin-loaded nanostructured lipid carriers as a tool in oral anti-mycobacterial treatment of crohn's disease. Nanomaterials 10, 1–18. https://doi.org/10.3390/nano10112138.

Sham, J.O.H., Zhang, Y., Finlay, W.H., Roa, W.H., Löbenberg, R., 2004. Formulation and characterization of spray-dried powders containing nanoparticles for aerosol delivery to the lung. Int. J. Pharm. 269, 457–467. https://doi.org/10.1016/j.ijpharm.2003.09.041.

Shanmuga Priya, A., Sivakamavalli, J., Vaseeharan, B., Stalin, T., 2013. Improvement on dissolution rate of inclusion complex of Rifabutin drug with β-cyclodextrin. Int. J. Biol. Macromol. 62, 472–480. https://doi.org/10.1016/j.ijbiomac.2013.09.006.

Singh, N., Sahoo, S.K., Kumar, R., 2020. Hemolysis tendency of anticancer nanoparticles changes with type of blood group antigen: an insight into blood nanoparticle interactions. Mater. Sci. Eng. C 109, 110645. https://doi.org/10.1016/j.msec.2020.110645.

Sosnik, A., Carcaboso, Á.M., Glisoni, R.J., Moretton, M.A., Chiappetta, D.A., 2010. New old challenges in tuberculosis: Potentially effective nanotechnologies in drug delivery. Adv. Drug Deliv. Rev. 62, 547–559. https://doi.org/10.1016/j.addr.2009.11.023.

Suárez, I., Fünger, S.M., Kröger, S., Rademacher, J., Fätkenheuer, G., Rybniker, J., 2019. The diagnosis and treatment of tuberculosis. Dtsch. Arztebl. Int. 116, 729–735. https://doi.org/10.3238/arztebl.2019.0729.

Tee, S.K., Marriott, C., Zeng, X.M., Martin, G.P., 2000. The use of different sugars as fine and coarse carriers for aerosolised salbutamol sulphate. Int. J. Pharm. 208, 111–123. https://doi.org/10.1016/S0378-5173(00)00553-6.

Thwala, L.N., Beloqui, A., Csaba, N.S., González-Touceda, D., Tovar, S., Dieguez, C., Alonso, M.J., Préat, V., 2016. The interaction of protamine nanocapsules with the intestinal epithelium: a mechanistic approach. J. Control. Release 243, 109–120. https://doi.org/10.1016/j.jconrel.2016.10.002.

Traini, D., Young, P.M., 2017. Drug delivery for tuberculosis: is inhaled therapy the key to success? Ther. Deliv. 8, 819–821. https://doi.org/10.4155/tde-2017-0050.

Vanhoorne, V., Van Bockstal, P.-J., Van Snick, B., Peeters, E., Monteyne, T., Gomes, P., De Beer, T., Remon, J.P., Vervaet, C., 2016. Continuous manufacturing of delta mannitol by cospray drying with PVP. Int. J. Pharm. 501, 139–147. https://doi.org/10.1016/j.ijpharm.2016.02.001.

Woods, A., Andrian, T., Sharp, G., Bicer, E.M., Vandera, K.-K.A., Patel, A., Mudway, I., Dailey, L.A., Forbes, B., 2020. Development of new *in vitro* models of lung protease activity for investigating stability of inhaled biological therapies and drug delivery systems. Eur. J. Pharm. Biopharm. 146, 64–72. https://doi.org/10.1016/j.ejpb.2019.11.005.

Yang, W., Peters, J.I., Williams, R.O., 2008. Inhaled nanoparticles—A current review. Int. J. Pharm. 356, 239–247. https://doi.org/10.1016/j.ijpharm.2008.02.011.

Zhang, Y., Huo, M., Zhou, J., Zou, A., Li, W., Yao, C., Xie, S., 2010. DDSolver: an add-in program for modeling and comparison of drug dissolution profiles. AAPS J. 12, 263–271. https://doi.org/10.1208/s12248-010-9185-1.